

**ENCLOSURE 1**

**CNRO-2004-00008**

**ARKANSAS NUCLEAR ONE, UNIT 1  
RELAXATION REQUEST #1**

**ENTERGY OPERATIONS, INC.  
ARKANSAS NUCLEAR ONE, UNIT 1**

**RELAXATION REQUEST #1 TO NRC ORDER EA-03-009**

**I. ASME COMPONENTS AFFECTED**

Arkansas Nuclear One, Unit 1 (ANO-1) has sixty-nine (69) ASME Class 1 reactor pressure vessel (RPV) head penetration nozzles comprised of sixty-eight (68) control rod drive mechanism (CRDM) nozzles and one (1) radiation calibration instrumentation nozzle. Of these nozzles, eight (8) were repaired during the previous refueling outage; two (2) using a weld overlay repair and six (6) using a pressure boundary relocation repair. See Figure 1 for penetration locations on the ANO-1 RPV head.

In accordance with Section IV.B of NRC Order EA-03-009 (the Order), the ANO-1 susceptibility category is "high" because of cracking experienced in RPV head penetration nozzles and J-groove welds due to primary water stress corrosion cracking (PWSCC).

This request does not apply to the eight previously repaired nozzles. As described in Footnote 3 of Section IV.B(1) of the Order, the six nozzles repaired using the pressure boundary relocation repair technique (#s 3, 6, 15, 17, 35, and 56) will be ultrasonically examined as specified in Request for Alternative ANO1-R&R-004, which was authorized by the NRC staff.<sup>1</sup> The two nozzles repaired using the weld overlay technique (#s 54 and 68) will be examined by performing either an eddy current testing (ECT) or liquid penetrant testing (PT) examination on the weld overlay and the inside diameter (ID) of the nozzle blind zone. (See Section III for a discussion of the blind zone.)

**II. NRC ORDER EA-03-009 APPLICABLE EXAMINATION REQUIREMENTS**

The NRC issued Order EA-03-009 that modified the current licenses at nuclear facilities utilizing pressurized water reactors (PWRs), which includes ANO-1. The Order establishes inspection requirements for RPV head penetration nozzles. ANO-1 is categorized as a "high" susceptibility plant as discussed above.

Section IV.C of the Order states in part:

"All Licensees shall perform inspections of the RPV head using the following techniques and frequencies:

- (1) For those plants in the High category, RPV head and head penetration nozzle inspections shall be performed using the following techniques every refueling outage.
  - (a) Bare metal visual examination of 100% of the RPV head surface (including 360° around each RPV head penetration nozzle), AND

---

<sup>1</sup> Letter from the NRC to Entergy Operations, Inc., *Arkansas Nuclear One, Unit No. 1 – RE: Relief Request to use Alternative Techniques for Reactor Pressure Vessel Closure Head Nozzles (TAC No. MB6599)*, dated November 25, 2003

- (b) Either:
  - (i) Ultrasonic testing of each RPV head penetration nozzle (i.e., nozzle base material) from two (2) inches above the J-groove weld to the bottom of the nozzle and an assessment to determine if leakage has occurred into the interference fit zone, OR
  - (ii) Eddy current testing or dye penetrant testing of the wetted surface of each J-groove weld and RPV head penetration nozzle base material to at least two (2) inches above the J-groove weld.”

### III. REASON FOR REQUEST

Section IV.F of the Order states:

“Licensees proposing to deviate from the requirements of this Order shall seek relaxation of this Order pursuant to the procedure specified below. The Director, Office of Nuclear Reactor Regulation, may, in writing, relax or rescind any of the above conditions upon demonstration by the Licensee of good cause. A request for relaxation regarding inspection of specific nozzles shall also address the following criteria:

- (1) The proposed alternative(s) for inspection of specific nozzles will provide an acceptable level of quality and safety, or
- (2) Compliance with this Order for specific nozzles would result in hardship or unusual difficulty without a compensating increase in the level of quality and safety.

“Requests for relaxation associated with specific penetration nozzles will be evaluated by the NRC staff using its procedure for evaluating proposed alternatives to the ASME Code in accordance with 10 CFR 50.55a(a)(3).”

Pursuant to Section IV.F(2) of the Order, Entergy Operations, Inc. (Entergy) requests relaxation from the requirements of Section IV.C(1)(b) for the 61 ANO-1 RPV head penetration nozzles that have not been repaired. Entergy plans to inspect these nozzles using the ultrasonic testing (UT) method in accordance with Section IV.C(1)(b)(i) of the Order to the maximum extent possible. However, a UT inspection of the ID of the RPV head nozzles at ANO-1 can only be performed from 2 inches above the J-groove weld down to a point approximately 0.516 inch above the bottom of the nozzle. This 0.516-inch “blind zone” is due to a limitation resulting from inspection probe design. This limitation and its associated hardship are discussed below in Section III.A.

Entergy also evaluated the impact of inspecting the blind zone of each RPV head penetration nozzle using either the liquid penetrant testing (PT) method or the eddy current testing (ECT) method as specified in Section IV.C(1)(b)(ii) of the Order. Entergy found hardship associated with these techniques, as discussed in Section III.B.

A. Inspection Probe Design Limitation

1. Description

The inspection probe to be used to inspect ANO-1 RPV head penetration nozzles consists of one (1) pair of ultrasonic time-of-flight diffraction (TOFD) transducers. The inspection probe is designed so that the ultrasonic transducers are slightly recessed into the probe holder. This recess must be filled with water to provide coupling between the transducer and the nozzle wall. Because of this design, the complete diameter of the transducer must fully contact the inspection surface before ultrasonic information can be collected. Based on probe configuration, the transducer pair only collects meaningful data down to a point approximately 0.516 inch above the bottom end of the nozzle. Below this point, meaningful UT data cannot be collected.

2. Hardship

Entergy knows of no UT equipment currently available that resolves the blind zone limitation; therefore, new UT equipment would have to be developed and appropriately qualified. The time and resources required to develop this equipment is unknown.

B. Hardship of Performing Alternative Surface Examinations

To perform either a PT or ECT inspection of the bottom end of each RPV head nozzle would result in a significant increase in personnel radiation exposure. Entergy estimates that the radiation exposure associated with performing the PT or ECT inspection to be approximately 0.16 man-REM per nozzle for a total exposure of 11 man-REM. In addition, Entergy estimates that to perform an examination on the entire wetted surface of each nozzle in accordance with Section IV.C(b)(1)(ii) of the Order would require additional under-head time for preparation and application resulting in approximately 26.5 to 27 man-REM total exposure.

In conclusion, Entergy can volumetrically inspect the RPV head nozzles in accordance with Section IV.C(1)(b)(i) of the Order from 2 inches above the weld to the top of the blind zone. Below this point, Entergy believes that the hardships associated with inspection activities required by the Order as discussed above are not commensurate with the level of increased safety or reduction in probability of leakage that would be obtained by complying with the Order.

IV. PROPOSED ALTERNATIVE AND BASIS FOR USE

Paragraph IV.C(1)(b)(i) of the Order requires that the UT inspection of each RPV head penetration nozzle encompass "from two (2) inches above the J-groove weld to the bottom of the nozzle." Due to the reasons stated in Section III above, Entergy requests relaxation from this requirement for the ANO-1 RPV head penetration nozzles and proposes an alternative, which involves the use of UT examination and analysis, as described below.

A. Proposed Alternative

1. UT Examination

The ID of each RPV head penetration nozzle (i.e., nozzle base material) shall be ultrasonically examined from two (2) inches above the weld to the blind zone portion above the bottom of the nozzle. In addition, an assessment to determine if leakage has occurred into the interference fit zone will be performed, as currently specified in Section IV.C(1)(b)(i) of the Order.

2. Analysis

For the blind zone portion of each RPV head penetration nozzle not examined by UT as required by the Order, analysis has been performed to determine if sufficient free-span lengths (uphill and downhill) exist between the blind zone and the weld to facilitate one (1) operating cycle of crack growth without the crack reaching the weld.

The analysis is summarized in Section IV.B.2 and is fully documented in Engineering Report M-EP-2004-001, Rev. 0 (Enclosure 2).

3. UT Verification of CRDM Nozzle 26

UT measurement data of the RPV head penetration nozzles obtained during the previous ANO-1 refueling outage was used to determine actual free-span lengths for the RPV head penetration nozzles. However, the storage data files containing the UT measurements for CRDM Nozzle 26 were found to be corrupted; therefore, its actual free-span lengths could not be determined. Because of this situation, Entergy will perform a UT examination on Nozzle 26 to determine its actual free-span lengths. If the free-span lengths meet the measured minimum free-span lengths for its associated nozzle group (26.2°) (see table in Section IV.B.2), no further actions will be required. If the free-span lengths fail to meet the lengths, Entergy will perform an augmented examination of the blind zone portion of Nozzle 26 not examined by UT. This examination will consist of either ECT or PT, or a combination of both techniques. If performed, this augmented inspection will be included in the 60-day report required by Section IV.E of the Order.

B. Basis for Use

The UT examination is the volumetric technique recognized in Section IV.C(1)(b)(i) of the Order. The proposed alternative includes the use of UT to the maximum extent practical based on the limits of current technology. However, because the technology cannot provide an inspection to the extent required by the Order (i.e., to the bottom of the nozzle), Entergy proposes supplemental analysis in addition to the UT examination. This approach provides a level of safety and quality commensurate with the intent of the Order. Each portion of the proposed alternative is discussed below.

## 1. UT Examination

Entergy will perform UT examination of the ANO-1 RPV head nozzles using the TOFD technique. The TOFD technique utilizes one pair of transducers aimed at each other looking in the axial direction of the penetration nozzle tube. One of the transducers sends sound into the inspection volume while the other receives the reflected and diffracted signals as they interact with the material. The TOFD technique is used to detect and characterize planar-type defects within the full volume of the tube.

The UT examination procedures and techniques to be utilized at ANO-1 have been satisfactorily demonstrated under the EPRI Materials Reliability Program (MRP) Inspection Demonstration Program.

## 2. Analysis

The extent of the proposed alternative is established by an engineering evaluation that includes a finite element stress analysis and fracture mechanics evaluations. The intent of the engineering evaluation is to determine whether sufficient free-span lengths (uphill and downhill) exist between the blind zone and the weld to facilitate one operating cycle of crack growth without the crack reaching the weld. See Figure 2.

Four (4) RPV head penetration nozzle locations have been selected for analysis in the engineering evaluation. The selected location groups (RPV head angles) are 0°, 18.2°, 26.2°, and 38.5° with the 0° head angle at the vertical centerline of the RPV head, the 38.5° head angle location being the outermost nozzles, and the other two groups being intermediate locations between the center and outermost locations.

As discussed in Section IV.A.3 above, Entergy evaluated UT measurement data obtained during the previous ANO-1 refueling outage to determine actual free-span lengths of the nozzles. The storage data files containing the UT measurements for CRDM Nozzle 26 were found to be corrupted; therefore, its actual free-span lengths could not be determined. As such, it could not be encompassed within this analysis.

The measured minimum free-span lengths for each nozzle group are documented in Table 1 of Engineering Report M-EP-2004-001 (Enclosure 2) and are summarized below. The analysis indicated that every nozzle, except CRDM Nozzle 26, has adequate free-span lengths. Actions to be taken for Nozzle 26 are discussed in Section IV.A.3.

Nozzle Group	Nozzle Numbers in the Group	Measured Minimum Free-Span Length @ Downhill Location	Measured Minimum Free-Span Length @ Uphill Location
0°	1	1.040 inches	1.040 inches
18.2°	2 thru 21	0.430 inch	1.450 inches
26.2°	22 thru 37	0.630 inch	2.840 inches
38.5°	38 thru 69	0.440 inch	3.080 inches

While evaluating the UT measurement data, Entergy discovered that the blind zone experienced during the previous nozzle examinations ranged from 0.589 inch to 1.818 inches depending on the specific nozzle location. This blind zone was due to (1) a limitation resulting from inspection probe design, and (2) probe lift-off encountered near the bottom of the nozzle while performing the UT examinations. With a redesign of the probe, the lift-off problems have been resolved. However, the probe design limitation is inherent to the technology. (See a discussion in Section III.A, above.) For conservatism, the analysis was performed using the larger blind zone lengths determined from the UT measurement data.

The results of the stress analysis at each location are bounding for nozzles higher on the head (e.g., analysis for 26.2° bounds the intermediate nozzles between 18.2° and 26.2°). The selected nozzle head angle locations provide an adequate representation of residual stress profiles and a proper basis for analysis to bound all RPV head nozzles. The stress analyses and fracture mechanics evaluations performed to address these conditions are summarized below.

#### Stress Analysis

A "finite element" based stress analysis (FEA) is performed on the ANO-1 RPV head nozzle locations in this evaluation. For conservatism, the yield strength used in the analysis for each nozzle head angle location is the highest yield strength of the RPV head penetration nozzles. To ensure that the FEA adequately modeled the as-built configuration of the ANO-1 CRDM nozzles and welds, a detailed review of actual UT examination data from the previous refueling outage was performed.

The FEA for the analyzed nozzles determines the stress distribution from the bottom of the nozzle to just above the top of the weld at the downhill, uphill, and mid-plane azimuthal locations. The downhill and mid-plane locations are selected for analysis because they represent the shortest distances that a crack has to propagate to reach the nozzle weld region. The uphill location is selected for completeness of the analysis. The results of the FEA are presented in Figures 4 through 17 and Tables 2 through 11 of Engineering Report M-EP-2004-001 (Enclosure 2). The stress distributions produced by this analysis are used to perform the fracture mechanics evaluations.

## Fracture Mechanics Evaluation

Safety analyses performed by the MRP have demonstrated that axial cracks in the nozzle tube material do not pose a challenge to the structural integrity of the nozzle. However, axial cracks may lead to pressure boundary leaks above the weld that could produce OD circumferential cracks and structural integrity concerns. Therefore, proper analysis of potential axial cracks in the blind zone of the RPV head nozzle is essential.

The analyses performed in the engineering evaluation are designed to determine the behavior of postulated cracks that could exist in the blind zone. Hence, the crack growth region is from the top of the blind zone to the bottom of the weld. The design review of the RPV head construction, the detailed residual stress analysis, selection of representative nozzle locations, utilization of representative fracture mechanics models, and the application of a suitable crack growth law provide a sound basis for the engineering evaluation.

Postulated cracks for the analysis include axial ID and OD part through-wall and through-wall cracks. Axial cracks are selected for evaluation in this analysis because of their potential to propagate to the weld region. Axial ID and OD part through-wall crack sizes were larger than twice the smallest crack sizes successfully detected by UT under the EPRI MRP Inspection Demonstration Program. Part through-wall cracks are centered at the top of the blind zone in the analysis. Through-wall cracks are postulated to exist from the top of the blind zone down to a point where the hoop stress is  $\leq 10$  ksi. The ID and OD part through-wall and through-wall cracks are located along the circumference of each nozzle at the 0° (downhill), 90° (mid-plane), and 180° (uphill) azimuthal locations, 0° (downhill) the furthest point from the center of the RPV head.

Thirty (30) different cases have been analyzed using crack growth rates from EPRI Report MRP-55, *Material Reliability Program – Crack Growth Rates for Evaluating Primary Water Stress Corrosion Cracking (PWSCC) of Thick-Wall Alloy 600 Material*. In summary, the evaluation results from all cases demonstrate that postulated flaws in the blind zone region will not compromise the weld in one cycle of operation. As previously discussed, CRDM Nozzle 26 will be volumetrically examined to ensure it meets this evaluation. The analysis further demonstrates that a larger margin exists (i.e. longer than one fuel cycle) at all evaluated locations. At several locations that were analyzed, no PWSCC-induced crack growth was observed because the stress distribution at these locations produced stress intensity factors that were below the threshold value for crack propagation by PWSCC. For the limited cases where PWSCC crack growth was predicted, the crack growth in one cycle of operation did not challenge the weld. Results of the fracture mechanics evaluations are documented in Table 14 of Engineering Report M-EP-2004-001 (Enclosure 2) and summarized below.

Nozzle Group	Azimuth Location	Crack Type	Allowed Propagation Dimension (inch) <sup>2</sup>	Allowed Growth/Cycle (inch) <sup>3</sup>
0°	All	ID	0.865 L / 0.617 D	0 L / 0 D
		OD	0.865	0
		Thru-wall	1.044	0
18.2°	Downhill	ID	0.255 L / 0.617 D	0.065 L / 0.111 D
		OD	0.255	0.062
		Thru-wall	0.430	0.313
	Uphill	ID	1.275 L / 0.617 D	0.032 L / 0.088 D
		OD	1.275	0
		Thru-wall	1.45	0
	Mid-plane	ID	0.96 L / 0.617 D	0 L / 0 D
		OD	0.96	0
		Thru-wall	1.135	0
26.2°	Downhill	ID	0.405 L / 0.617 D	0.041 L / 0.092 D
		OD	0.405	0
		Thru-wall	0.58	0
	Uphill	ID	2.665 L / 0.617 D	0 L / 0 D
		OD	2.665	0
		Thru-wall	2.84	0
	Mid-plane	ID	1.645 L / 0.617 D	0 L / 0 D
		OD	1.645	0
		Thru-wall	1.82	0
38.5°	Downhill	ID	0.265 L / 0.617 D	0 L / 0 D
		OD	0.265	0.010
		Thru-wall	0.44	0
	Uphill	ID	2.905 L / 0.617 D	0 L / 0 D
		OD	2.905	0
		Thru-wall	3.08	0
	Mid-plane	ID	1.805 L / 0.617 D	0 L / 0 D
		OD	1.805	0
		Thru-wall	1.98	0

<sup>2</sup> L = Length; D = Depth

<sup>3</sup> Both L and D dimensions are given for surface cracks on the ID. The limiting condition is reached when the postulated crack becomes through-wall and the upper tip reaches the bottom of the weld. The allowable propagation length of the surface-connected crack, L, is equal to the actual (measured) free-span length minus 0.175 inch, which is the distance the crack extends into the free-span at the minimum detectable crack size.

### Additional Analyses

The fracture mechanics evaluations described above assess the potential for postulated cracks to propagate from the top of the blind zone to the weld in less than one cycle of plant operation, assuming either an ID or OD crack with an initial length of approximately two (2) times the smallest detectable length, or a through-wall crack from the top of the blind zone down to a point where the hoop stress is  $\leq 10$  ksi. Because the blind zone is significantly longer than the smallest detectable length, this approach did not consider ID or OD cracks that extend down to the bottom of the nozzle. This is appropriate if the hoop stress at the bottom of the postulated flaw is compressive or if the hoop stress is a low tensile stress ( $< 10$  ksi), as these hoop stresses will not propagate PWSCC. For the through-wall cracks, in all cases, the hoop stress rapidly decreases below the blind zone such that none of the postulated through-wall cracks extend to the bottom of the nozzle.

The potential for postulated cracks to propagate from the bottom of the blind zone to the weld was also evaluated. In general, the stress analysis indicates that the magnitude of the hoop stress distribution from the top of the blind zone to the bottom of the nozzle along both the ID and OD surfaces decreases steadily and becomes compressive. The extent or height of the compression zone for each nozzle group and azimuthal location is presented in Table 13 of the Engineering Report M-EP-2004-001 (Enclosure 2) and is summarized below.

Nozzle Group	Azimuthal Location	Compression Zone Height	Maximum Hoop Stress Where No Compression Zone Exists
0°	All	0.56 inch	N/A
18.2°	Downhill	0.4 inch	N/A
	Uphill	0.8 inch	N/A
	Mid-plane	0.9 inch	N/A
26.2°	Downhill	0.357 inch	N/A
	Uphill	0.953 inch	N/A
	Mid-plane	0.875 inch	N/A
38.5°	Downhill	0.5 inch	N/A
	Uphill	1.0 inch	N/A
	Mid-plane	0	10.954 ksi

The height of the compression zone is measured from the bottom of the nozzle. Within the compression zone regions, no PWSCC-assisted crack growth is possible. For those nozzle groups with a tensile stress below 10 ksi, the possibility for PWSCC crack initiation is extremely low. Based on these stress profiles, only the 38.5° mid-plane location warrants additional analysis for crack growth below the postulated cracks discussed above.

A hoop stress of 10.954 ksi exists along the ID surface at the bottom of the 38.5° nozzle at the mid-plane location. Because of this higher stress value, this nozzle location was selected for additional analysis by fracture mechanics. An ID surface crack was postulated near the bottom of the nozzle. The analysis showed that it would not propagate from PWSCC. However, the model for the surface crack is based on cracks that are remote from the edge of the plate. Because of this, a through-wall edge crack at the bottom of the nozzle was also evaluated. Based on this analysis, postulated cracks at the bottom of the 38.5° nozzle (mid-plane) do not propagate into the weld in less than one cycle of plant operation was evaluated. Furthermore, the analysis results indicate that the postulated cracks in the region do not reach the weld in two (2) years of operation. For additional details, see the Additional Analysis subsection of Section 5.0 in Engineering Report M-EP-2004-001 (Enclosure 2).

#### Analysis Conclusions

Fracture mechanics evaluations were performed at the downhill, uphill, and mid-plane locations of the 0°, 18.2°, 26.2°, and 38.5° RPV head nozzles to assess the potential for postulated cracks to grow from the blind zone to the nozzle weld in less than one cycle of plant operation. Additional analyses were performed to assess the potential for postulated cracks to grow from along the bottom of the 38.5° nozzle at the mid-plane location to the weld in one cycle of operation.

The evaluations indicate that a crack in the blind zone of a nozzle will not grow into the weld of the nozzle within one cycle of operation. See Table 1 which identifies the nozzle locations bounded by these evaluations. For details regarding the engineering evaluation and its conclusions, see Engineering Report M-EP-2004-001 (Enclosure 2).

This analysis incorporates a crack-growth formula different from that described in Footnote 1 of the Order, as provided in EPRI Report MRP-55. Entergy is aware that the NRC staff has not yet completed a final assessment regarding the acceptability of the EPRI report. If the NRC staff finds that the crack-growth formula in MRP-55 is unacceptable, Entergy shall revise its analysis that justifies relaxation of the Order within 30 days after the NRC informs Entergy of an NRC-approved crack-growth formula. If Entergy's revised analysis shows that the crack growth acceptance criteria are exceeded prior to the end of Operating Cycle 19 (following the upcoming refueling outage), Entergy will, within 72 hours, submit to the NRC written justification for continued operation. If the revised analysis shows that the crack growth acceptance criteria are exceeded during the subsequent operating cycle, Entergy shall, within 30 days, submit the revised analysis for NRC review. If the revised analysis shows that the crack growth acceptance criteria are not exceeded during either Operating Cycle 19 or the subsequent operating cycle, Entergy shall, within 30 days, submit a letter to the NRC confirming that its analysis has been revised. Any future crack-growth analyses performed for Operating Cycle 19 and future cycles for RPV head penetrations will be based on an NRC-acceptable crack growth rate formula.

### 3. UT Verification of CRDM Nozzle 26

As stated in Section IV.A.3, above, the data files containing UT measurements for CRDM Nozzle 26 were corrupted thereby preventing Entergy from determining its actual free-span lengths. By performing a UT examination to verify that the free-span lengths of the nozzle meet the acceptance criteria, Entergy will demonstrate that an undetected crack in the blind zone will not reach the nozzle's J-groove weld within one (1) operating cycle.

In the event that a free-span length does not meet its acceptance criterion, the augmented examination of the blind zone ensures that a crack within the blind zone will be detected.

## V. CONCLUSION

Section IV.F of the Order states:

"Licensees proposing to deviate from the requirements of this Order shall seek relaxation of this Order pursuant to the procedure specified below. The Director, Office of Nuclear Reactor Regulation, may, in writing, relax or rescind any of the above conditions upon demonstration by the Licensee of good cause. A request for relaxation regarding inspection of specific nozzles shall also address the following criteria:

- (1) The proposed alternative(s) for inspection of specific nozzles will provide an acceptable level of quality and safety, or
- (2) Compliance with this Order for specific nozzles would result in hardship or unusual difficulty without a compensating increase in the level of quality and safety."

Section IV.C(1)(b) of the Order establishes a minimum set of RPV head penetration nozzle inspection requirements to identify the presence of cracks in penetration nozzles that could lead to leakage of reactor coolant and wastage of RPV head material.

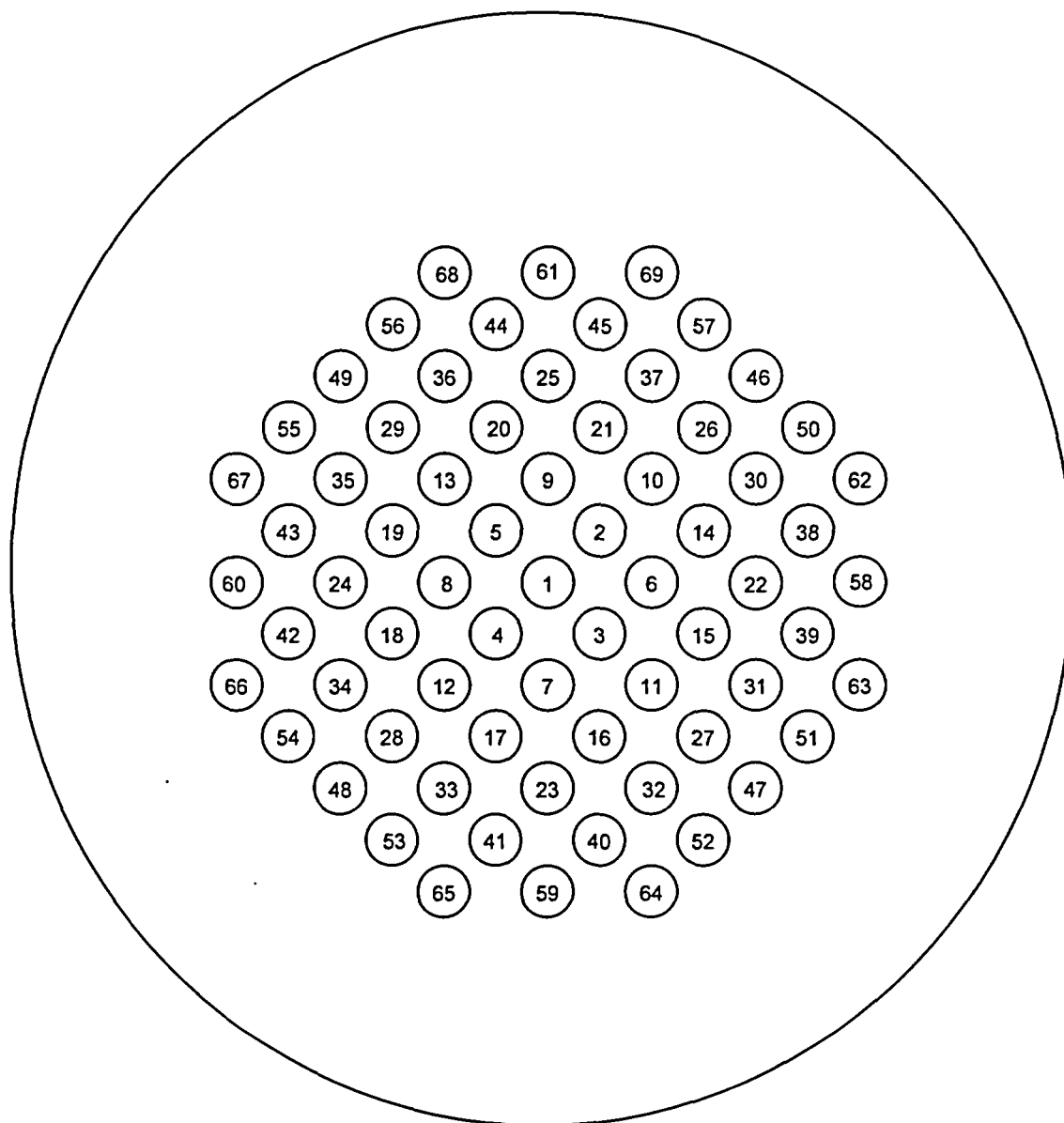
Entergy believes that compliance with the UT inspection provisions of Section IV.C(1)(b)(i) of the Order as described in Section II above would result in hardships and unusual difficulties, as discussed in Section III above, without a compensating increase in the level of quality and safety.

Entergy believes the proposed alternative, described in Section IV, provides an acceptable level of quality and safety by utilizing inspections and analysis to determine the condition of the ANO-1 RPV head penetration nozzles. The technical basis for the analysis of the proposed alternative is documented in Engineering Report M-EP-2004-001, Rev. 0, which is contained in Enclosure 2 of this letter. Entergy believes that by employing analytical and inspection techniques, the two-step proposed alternative provides an adequate process for inspecting, evaluating, and determining the condition of the ANO-1 RPV head penetration nozzles with regard to the presence of PWSCC. Entergy concludes that the proposed alternative adequately meets the intent of the Order. Therefore, we request that the NRC staff authorize the proposed alternative pursuant to Section IV.F of the Order.

**TABLE 1**

**Results of Crack Growth Analysis**

<b>Nozzle Location</b>	<b>Nozzle Azimuth Location</b>	<b>Axial Crack Evaluated</b>	<b>Crack Evaluation Results</b>
0°	All	ID Part through-wall	No PWSCC growth
		OD Part through-wall	No PWSCC growth
		Through-wall	No PWSCC growth
18.2°	Downhill	ID Part through-wall	Greater than 1 Cycle to reach weld
		OD Part through-wall	Greater than 1 Cycle to reach weld
		Through-wall	Greater than 1 Cycle to reach weld
	Uphill	ID Part through-wall	No PWSCC growth
		OD Part through-wall	No PWSCC growth
		Through-wall	No PWSCC growth
	Mid-plane	ID Part through-wall	No PWSCC growth
		OD Part through-wall	No PWSCC growth
		Through-wall	No PWSCC growth
26.2°	Downhill	ID Part through-wall	Greater than 1 Cycle to reach weld
		OD Part through-wall	No PWSCC growth
		Through-wall	Greater than 1 Cycle to reach weld
	Uphill	ID Part through-wall	No PWSCC growth
		OD Part through-wall	No PWSCC growth
		Through-wall	No PWSCC growth
	Mid-plane	ID Part through-wall	No PWSCC growth
		OD Part through-wall	No PWSCC growth
		Through-wall	No PWSCC growth
38.5°	Downhill	ID Part through-wall	No PWSCC growth
		OD Part through-wall	Greater than 1 Cycle to reach weld
		Through-wall	No PWSCC growth
	Uphill	ID Part through-wall	No PWSCC growth
		OD Part through-wall	No PWSCC growth
		Through-wall	No PWSCC growth
	Mid-plane	ID Part through-wall	No PWSCC growth
		OD Part through-wall	No PWSCC growth
		Through-wall	No PWSCC growth



RPV Head Penetration Nozzles

Radiation Calibration Instrument nozzle: 1

CRDM nozzles: 2 - 69

Previously Repaired Nozzles

Weld Overlay: 54 and 68

Pressure Boundary Relocation: 3, 6, 15, 17, 35, & 56

**FIGURE 1**

**CRDM NOZZLE LOCATIONS ON THE ANO-1 RPV HEAD**

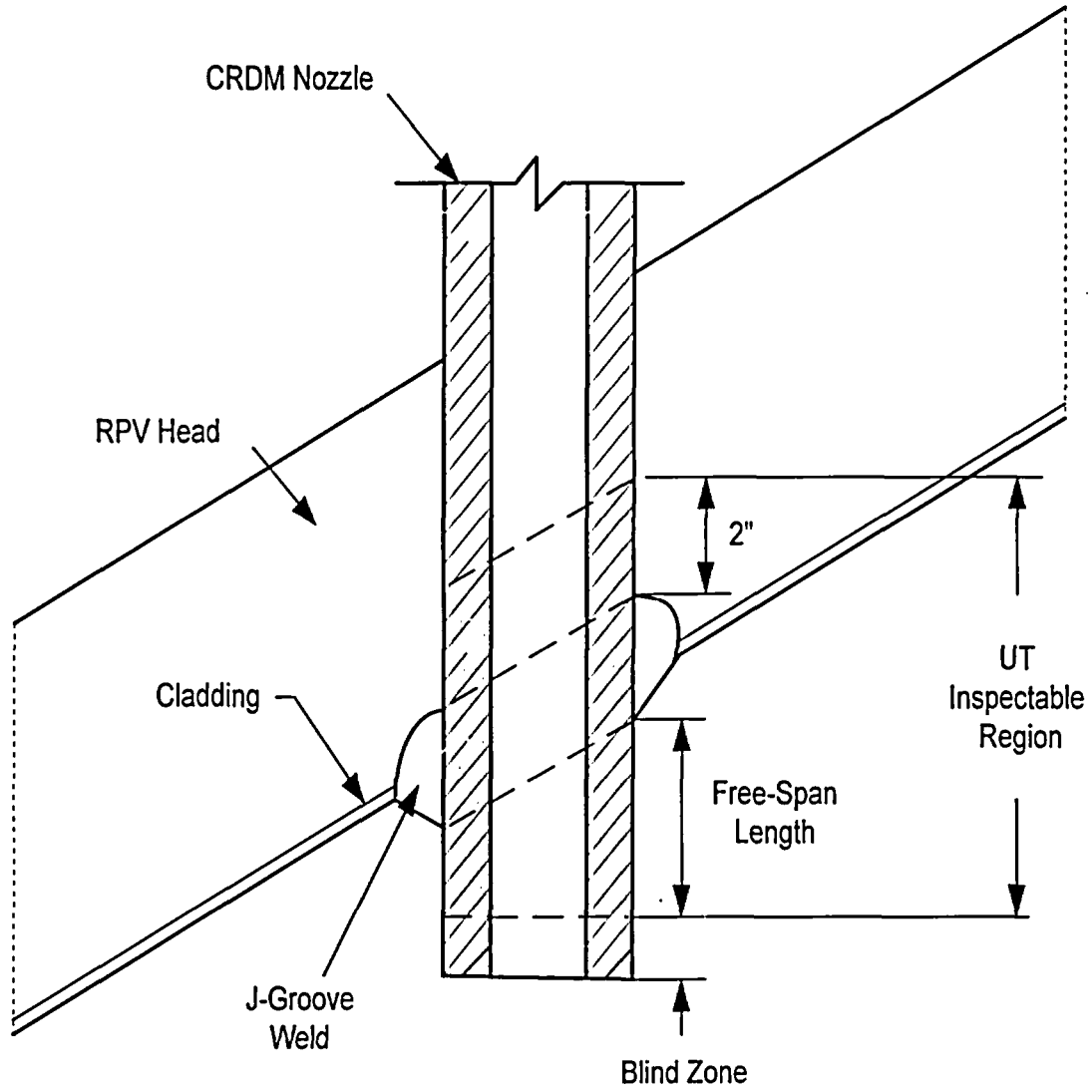


**FIGURE 2**  
**CRDM NOZZLE CONFIGURATION**

**ENCLOSURE 2**

**CNRO-2004-00008**

**ENGINEERING REPORT M-EP-2004-001, REV. 0**

***FRACTURE MECHANICS ANALYSIS FOR THE ASSESSMENT OF THE  
POTENTIAL FOR PRIMARY WATER STRESS CORROSION CRACK (PWSCC)  
GROWTH IN THE UNINSPECTED REGIONS OF THE  
REACTOR PRESSURE VESSEL HEAD NOZZLES AT  
ARKANSAS NUCLEAR ONE, UNIT 1***



**ENERGY NUCLEAR SOUTH**  
**Engineering Report Coversheet**

**Fracture Mechanics Analysis for the Assessment  
 of the  
 Potential for Primary Water Stress Corrosion Crack (PWSCC) Growth  
 in the  
 Un-Inspected Regions of the Control Rod Drive Mechanism (CRDM) Nozzles  
 at  
 Arkansas Nuclear One Unit 1**

**Engineering Report Type:**

New  Revision Deleted  Superseded

**Applicable Site(s)**

ANO  Echelon  GGNS  RBS  WF3

Report Origin:  ENS  Vendor Safety-Related:  Yes  No

Vendor Document No. \_\_\_\_\_

Prepared by:	<u>J.S. Rothman</u> Responsible Engineer	Date: <u>1/29/04</u>	Comments: <input type="checkbox"/> Yes <input type="checkbox"/> No	Attached: <input type="checkbox"/> Yes <input type="checkbox"/> No
Verified/ Reviewed by:	<u>Brian C. Gray</u> Design Verifier/Reviewer	Date: <u>1/29/04</u>	<input checked="" type="checkbox"/> Yes <input type="checkbox"/> No	<input type="checkbox"/> Yes <input checked="" type="checkbox"/> No
Approved by:	<u>R. S. [Signature]</u> Responsible Supervisor or Responsible Central Engineering Manager (for multiple site reports only)	Date: <u>2/2/04</u>	<input type="checkbox"/> Yes <input checked="" type="checkbox"/> No	<input type="checkbox"/> Yes <input checked="" type="checkbox"/> No

E-M-EP-2004-001      00

Engineering Report No. \_\_\_\_\_ Rev. \_\_\_\_\_

Page 2 of 54

**RECOMMENDATION FOR APPROVAL FORM**

		Comments:	Attached:
Prepared by: <u>J.S. Richardson</u> Responsible Engineer	Date: <u>1/28/04</u>	<input type="checkbox"/> Yes <input type="checkbox"/> No	<input type="checkbox"/> Yes <input type="checkbox"/> No
Concurrence: <u>[Signature]</u> Responsible Engineering Manager, ANO	Date: <u>1/29/04</u>	<input type="checkbox"/> Yes <input checked="" type="checkbox"/> No	<input type="checkbox"/> Yes <input checked="" type="checkbox"/> No
Concurrence: _____ Responsible Engineering Manager, GGNS	Date: _____	<input type="checkbox"/> Yes <input type="checkbox"/> No	<input type="checkbox"/> Yes <input type="checkbox"/> No
Concurrence: _____ Responsible Engineering Manager, RBS	Date: _____	<input type="checkbox"/> Yes <input type="checkbox"/> No	<input type="checkbox"/> Yes <input type="checkbox"/> No
Concurrence: _____ Responsible Engineering Manager, WF3	Date: _____	<input type="checkbox"/> Yes <input type="checkbox"/> No	<input type="checkbox"/> Yes <input type="checkbox"/> No

## Table of Contents

Section	Title	Page Number
	List of Tables	3
	List of Figures	4
	List of Appendices	5
1.0	Introduction	6
2.0	Stress Analysis	10
3.0	Analytical Basis for Fracture Mechanics and Crack Growth Models	26
4.0	Method of Analysis	31
5.0	Discussion and Results	36
6.0	Conclusions	52
7.0	References	54

## List of Tables

Table Number	Title	Page Number
1	Minimum freespan length for the nozzle group used in the current evaluation.	9
2	Nodal Stress data for 0° Nozzle.	16
3	Nodal Stress data for the 18.2° nozzle at the downhill location.	17
4	Nodal Stress data for the 18.2° nozzle at the uphill location	18
5	Nodal Stress data for the 18.2° nozzle at the mid-plane location.	19
6	Nodal Stress data for the 26.2° nozzle at the downhill location.	20
7	Nodal Stress data for the 26.2° nozzle at the uphill location.	21
8	Nodal Stress data for the 26.2° nozzle at the mid-plane location.	22
9	Nodal Stress data for the 38.5° nozzle at the downhill location.	23
10	Nodal Stress data for the 38.5° nozzle at the uphill location.	24
11	Nodal Stress data for the 38.5° nozzle at the mid-plane location.	25
12	Comparison of Fracture Mechanics Models	41
13	Results for compression zone	42
14	ANO-1 Estimated As-Built Analyses Results Summary	44

## List of Figures

Figure Number	Title	Page Number
1	Sketch showing CRDM penetration	7
2	Sketch of a typical inspection probe sled [3a].	8
3	Finite element model of the 38.5° nozzle	11
4	Hoop Stress contours for the 0° nozzle.	13
5	Hoop Stress contours for the 18.2° nozzle.	13
6	Hoop Stress contours for the 26.2° nozzle.	14
7	Hoop Stress contours for the 38.5° nozzle.	14
8	Plot showing hoop stress distribution along tube axis for the 0° nozzle.	16
9	Plot showing hoop stress distribution along tube axis for the 18.2° nozzle at the downhill location.	17
10	Plot showing hoop stress distribution along tube axis for the 18.2° nozzle at the uphill location.	18
11	Plot showing hoop stress distribution along tube axis for the 18.2° nozzle at mid-plane location.	19
12	Plot showing hoop stress distribution along tube axis for the 26.2° nozzle at the downhill location.	20
13	Plot showing hoop stress distribution along tube axis for the 26.2° nozzle at the uphill location.	21
14	Plot showing hoop stress distribution along tube axis for the 26.2° nozzle at the mid-plane location.	22
15	Plot showing hoop stress distribution along tube axis for the 38.5° nozzle at the downhill location.	23
16	Plot showing hoop stress distribution along tube axis for the 38.5° nozzle at the uphill location..	24
17	Plot showing hoop stress distribution along tube axis for the 38.5° nozzle at the mid-plane location.	25
18	SICF shown as a function of normalized crack depth for the "a-tip" and the "c-tip"	27
19	Curve fit equations for the "extension and bending" components in Reference 6.	30
20	Plots showing effect of nodal data selection on the accuracy of polynomial regression fit,	34
21	Comparison of SICF for the edge crack configurations with the membrane SICF for current model.	39
22	Comparison of SIF for the current model and conventional model.	40
23	SIF comparison between current model and conventional model.	40

**List of Figures (Continued)**

<b>Figure Number</b>	<b>Title</b>	<b>Page Number</b>
24	ID surface crack for nozzle group 18.2° at downhill location.	45
25	OD surface crack for nozzle group 18.2° at downhill location.	46
26	Through-wall crack for nozzle group 18.2° at downhill location.	46
27	ID surface crack for nozzle group 18.2° at uphill location.	47
28	ID surface crack for nozzle group 26.2° at downhill location.	48
29	Through-wall crack for nozzle group 26.2° at downhill location.	48
30	OD surface crack for nozzle group 38.5° at downhill location.	49
31	Nozzle group 38.5° at mid-plane location.	50
32	Nozzle group 38.5° at mid-plane location ID surface crack.	51
33	Nozzle group 38.5° at mid-plane location with an edge crack.	52

**List of Appendices**

<b>Appendix Number</b>	<b>Content of Appendix</b>	<b>Number of Attachments in Appendix</b>
A	Design Information and UT analysis results,	2
B	Mathcad worksheets annotated to describe the three models	3
C	Mathcad worksheets for ANO-1 Analyses	32
D	Verification and Comparisons (Mathcad worksheets)	6

## 1.0 Introduction

The US Nuclear Regulatory Commission (NRC) issued Order EA-03-009 [1], which modified licenses, requiring inspection reactor vessel head (RVH) penetrations, which includes Control Rod Drive Mechanism (CRDM) penetrations at nuclear facilities utilizing pressurized water reactors (PWRs). Paragraph IV.C.1.b of the Order requires the inspection to cover a region from the bottom of the nozzle to two (2.0) inches above the J-groove weld. In the Babcock & Wilcox (B&W) reactor vessel design the CRDM nozzles are tubular penetrations into RVH that are joined to the RVH by a J-groove weld. The typical CRDM connection is shown in Figure 1. The design of the ultrasonic testing (UT) probes results in a region above the bottom of the nozzle (shown in Figure 1 as "blind zone") that cannot be inspected. Therefore, the region of the CRDM base metal that can be inspected begins above the blind zone and extends to two (2.0) inches above the J-groove weld. The unexamined length (here after called the blind zone) was obtained from a review of the UT data from the previous inspection campaign. From this review the highest value for the blind zone for a group of nozzles was used in the current analysis. The terms used in this report are defined as follows:

- Freespan = (bottom of weld – blind zone); this area below the weld is accessible for volumetric examination.
- Available Propagation Length = (bottom of weld –top of crack tip); area available for crack growth.

*Note: For an outside diameter (OD) surface crack, this length is always less than the freespan; for through-wall it is equal to the freespan; and, for an inside diameter (ID) surface crack, the criterion is the propagation length and a through-wall penetration condition.*

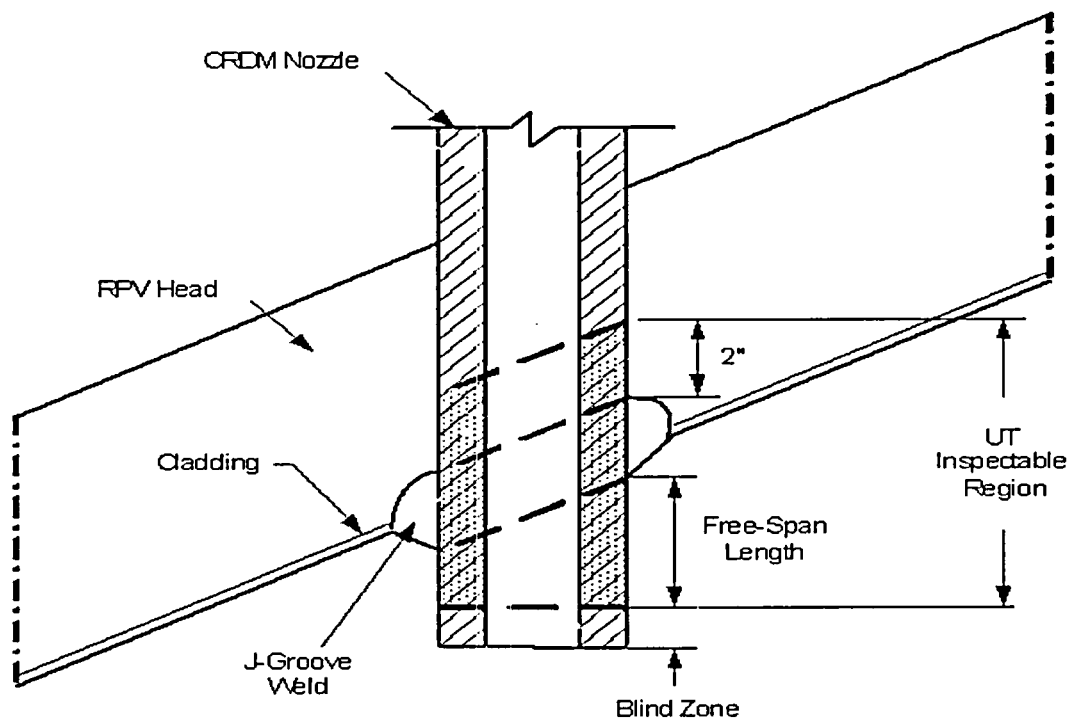
The nozzle as-built dimensions were determined by a detailed review of UT data from the previous inspection and design information for Arkansas Nuclear One Unit 1 (ANO-1), which are documented in Appendix "A". The finite element model to obtain the prevailing stress distributions (Residual+Operating) that are to be used in the deterministic fracture mechanics analyses were obtained from the analysis that were performed to support the inspection campaign during the previous refueling outage. The deterministic fracture mechanics analyses, in turn, assess the potential for primary water stress corrosion cracking (PWSCC) in the blind zone of the nozzles. The details of the stress analysis including the finite element models are discussed in Section 2. The UT data from Arkansas Nuclear One Unit 1 (ANO-1) was used to establish the available freespan length, which are documented in Appendix "A".

In order to exclude the blind zone from the inspection campaign, a relaxation of the Order is required pursuant to the requirements prescribed in Section IV.F and footnote 2 of the Order [1].

The purpose of this engineering report is to provide detailed analyses to support a relaxation request. The work plan developed for the analyses were as follows:

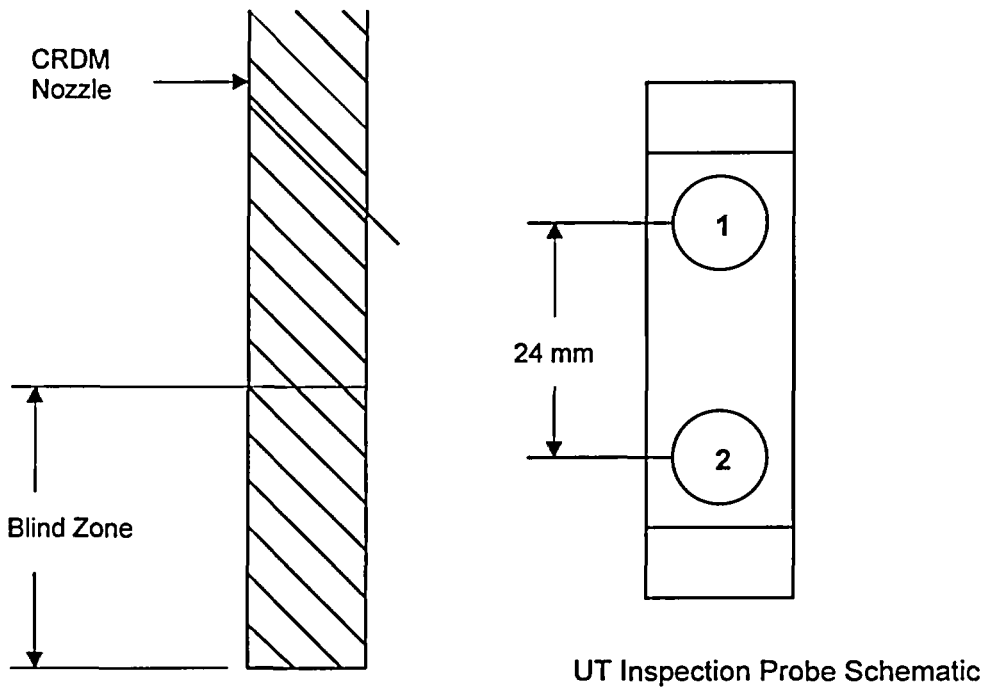
1. Determine if sufficient propagation length between the blind zone and the weld exists to facilitate one (1) cycle of axial crack growth without the crack reaching the weld; and,
2. For nozzles not meeting 1 above, determine how much of the blind zone combined with the available freespan is required to facilitate one (1) cycle of crack growth without the crack reaching the weld. This area is subject to augmented surface examination.

Figure 1 below shows the general arrangement of the CRDM nozzles with connection details. In this figure the various regions are defined. This figure provides a general overview of the CRDM penetration and the regions planned for volumetric inspection, and the regions that cannot be inspected (blind zone) by the volumetric UT method.



**Figure 1:** Sketch showing a CRDM penetration. Typical freespan is shown on the downhill side, the freespan length on the uphill side would be considerably larger. The blind zone, based on inspection probe design is also shown.

The UT blind zone, determined to be approximately 0.400 inch above the bottom of the nozzle, is based on a typical inspection probe sled design (shown in Figure 2). However, based on the previous refueling outage inspections, the measured freespan indicated a larger blind zone to exist. This was attributed to the lift-off effect at the bottom of the nozzle. In the current analysis the shortest measured freespan for each nozzle group was used to establish the blind zone. The UT data analysis results are documented in Attachment 2 of Appendix "A".



See table below for transducer information.

Position	Mode	Diameter	Description
1	Transmit	0.25 inch	Axial Scan Using TOFD
2	Receive	0.25 inch	Axial Scan Using TOFD

Figure 2: Sketch of a typical inspection probe sled. The blind zone indicated on the sketch was determined from an analysis of the UT inspection data obtained from the inspection performed during the previous refueling outage.

The residual stress analysis, discussed in the next section, was performed for four nozzle groups to represent the various nozzle penetration head angles. The UT analysis results (Appendix "A") was reviewed and the minimum freespan length for each of the nozzle groups is shown in Table 1 below.

Nozzle Group Penetration Angle (Degrees)	Nozzle Number In the Group	Minimum Freespan Length @ Downhill Location (inch)	Minimum Freespan Length @ Uphill Location (inch)
0	1	1.040	1.040
18.2	2 through 21	0.430	1.450
26.2	22 through 37	0.580	2.840
38.5	38 through 69	0.440	3.080

**Table 1:** Minimum freespan length for the nozzle group used in the current evaluation.

The analysis applied to determine the impact of not examining the blind zone independently evaluates a part through-wall axial crack initiated from the ID, a part through-wall axial crack initiated from the OD, and a through-wall axial crack.

#### Part Through-Wall Cracks

The initial crack depth obtained from Reference 2 is 11.0% of wall thickness deep for an ID axial crack and 16% of wall thickness deep for an OD axial crack. The crack length is based on the detected length of 4 mm (0.157 inch) from Reference 2. In the deterministic fracture mechanics analyses, the part through-wall crack lengths are more than doubled to 0.35 inch and the crack center is located at the top of the blind zone. Thus, the crack spans both the blind zone and the inspectable region. The postulated crack sizes and depths are two times the detectable limits with one-half (0.175 inch) of the flaw length being located in the examinable area. This provides for a conservative evaluation because:

- A) By extending the postulated crack 0.175 inch into the inspectable region, it places the crack tip closer to the weld where the hoop stresses are higher; and
- B) It assumes that 0.175 inch of the inspectable region is already cracked, reducing the remaining area for crack propagation.

#### Through-Wall Crack

In addition to evaluating the part through-wall cracks, this evaluation also conservatively evaluates a through-wall axial crack. The through-wall axial

crack is postulated to exist from the top of the blind zone down to a point where the hoop stress is  $\leq 10$  ksi. This is a very conservative assumption, since for a crack to initiate on the surface and propagate through-wall while being totally contained within the blind zone would result in an unrealistic aspect ratio. As can be concluded from the following analysis, the length of a part through-wall crack would propagate into the inspectable region long before its depth reaches a through-wall condition. However, evaluation of the through-wall crack provides completeness to this assessment and ensures all plausible crack propagation modes are considered. Like the part through-wall crack, the hoop stresses at the top of the blind zone were used as the initial stress with adjustments to account for the increased stresses as the crack approaches the weld.

The analyses include a finite element stress analysis of the CRDM nozzles and a fracture mechanics-based crack growth analysis for PWSCC. These analyses are performed for four nozzles (the nozzles were chosen at four head angles;  $0^\circ$ ,  $18.2^\circ$ ,  $26.2^\circ$ , and  $38.5^\circ$ ) in the reactor vessel head to account for the varied geometry of the nozzle penetration. In this manner the analysis provides a bounding evaluation for all CRDM nozzles in the reactor vessel head. The sections that follow contain a description of the analyses, the results, and conclusions supported by the analyses.

## 2.0 Stress Analysis

The residual stress existing in the nozzle at the J-groove weld has been extensively studied [3a]. These studies show that the residual stresses present in the nozzle tube are sufficiently high to warrant analysis for PWSCC induced crack growth. The propensity for PWSCC initiation and propagation depends on the residual stress distribution and its magnitude. Therefore, finite element-based stress analyses for ANO-1 CRDM penetrations using the highest tensile yield strength were performed [3b]. The nozzle groups considered were  $0^\circ$ ,  $18.2^\circ$ ,  $26.2^\circ$ , and  $38.5^\circ$ . The dimensions for the model were obtained from ANO-1 design drawings that are documented in Reference 3b. The finite element model of the  $38.5^\circ$  nozzle is shown in Figure 3. The models for the other nozzle groups were constructed in a similar manner. The model defines one half of the full nozzle since the nozzle is symmetrical about a vertical plane that bisects the nozzle along a line drawn from the downhill to uphill location. Fine mesh was used in the critical regions of the J-groove weld. The nozzle tube wall was modeled with four elements in the thickness direction. Thus the stress distribution across the wall could be accurately estimated. The RVH surrounding the nozzle was modeled in sufficient detail to account for the interaction between the nozzle and the RVH.

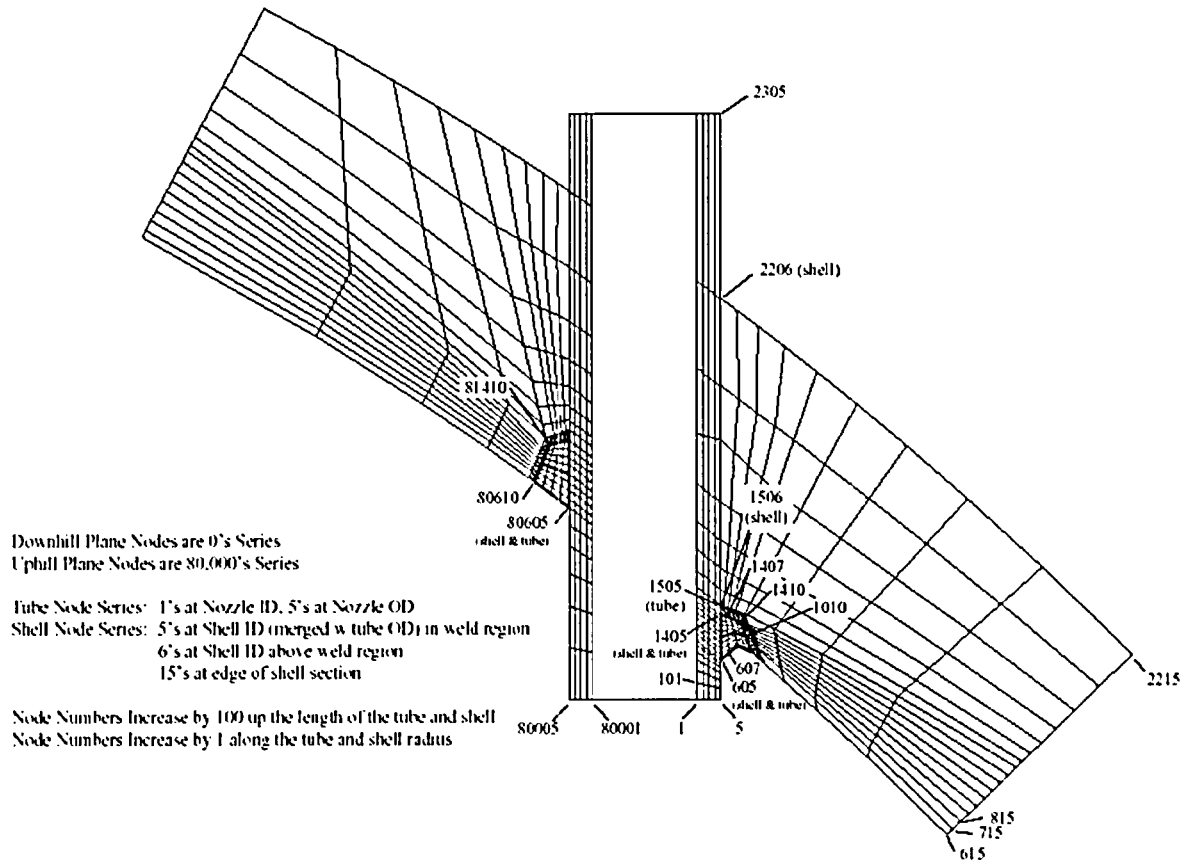


**Figure 3:** Finite element model of the 38.5° nozzle. Fine mesh geometry at the location of interest can be noted. Sufficient region of the RVH, surrounding the nozzle, is incorporated to ensure the accuracy of the analyses.

The finite element modeling for obtaining the necessary stress (residual+operating) distribution for use in fracture mechanics analysis followed the process and methodology described in Reference 3a. The modeling steps were as follows:

- 1) The finite element mesh consisted of 3-dimensional solid (brick) elements. Four elements were used to model the tube wall and similar refinement was carried to the attaching J-weld.
- 2) The CRDM tube material was modeled with a monotonic stress-strain curve. The highest yield strength from the nozzle material bounded by the nozzle group was used. This yield strength was referenced to the room temperature yield strength of the stress-strain curve described in Reference 5a. The temperature dependent stress-strain curves were obtained by

indexing the temperature dependent drop of yield strength.

- 3) The weld material was modeled as elastic-perfectly plastic for the weld simulation. This approximation is considered reasonable since most of the plastic strain in the weld metal occurs at high temperatures where metals do not work-harden significantly (Reference 3c). The temperature in the weld is high during the welding process. Once the weld begins to cool, the temperatures in the weld at which strain hardening would persist are of limited duration (Reference 3c). This was borne out by the comparison between the analysis based residual stress distribution and that obtained from experiments (Reference 3d).
- 4) The weld is simulated by two passes based on studies presented in Reference 3a.
- 5) After completing the weld, a simulated hydro-test load step is applied to the model. The hydro-test step followed the fabrication practice.
- 6) The model is then subjected to a normal operating schedule of normal heat up to steady state conditions at operating pressure. The residual plus operating stresses, once steady state has been achieved, are obtained for further analysis. The nodal stresses of interest are stored in an output file. These stresses are then transferred to an Excel spreadsheet for use in fracture mechanics analysis [3b].

The stress contours for the four nozzle groups obtained from the finite element analysis are presented in Figures 4 through 7. The stress contour color scheme is as follows:

<b>Dark Navy blue</b>	<i>from Minimum (Compression) to -10 ksi</i>
<b>Royal blue</b>	<i>from -10 to 0 ksi</i>
<b>Light blue</b>	<i>from 0 to 10 ksi</i>
<b>Light green</b>	<i>from 10 to 20 ksi</i>
<b>Green</b>	<i>from 20 to 30 ksi</i>
<b>Yellow green</b>	<i>from 30 to 40 ksi</i>
<b>Yellow</b>	<i>from 40 to 50 ksi</i>
<b>Red</b>	<i>from 50 to 100 ksi</i>

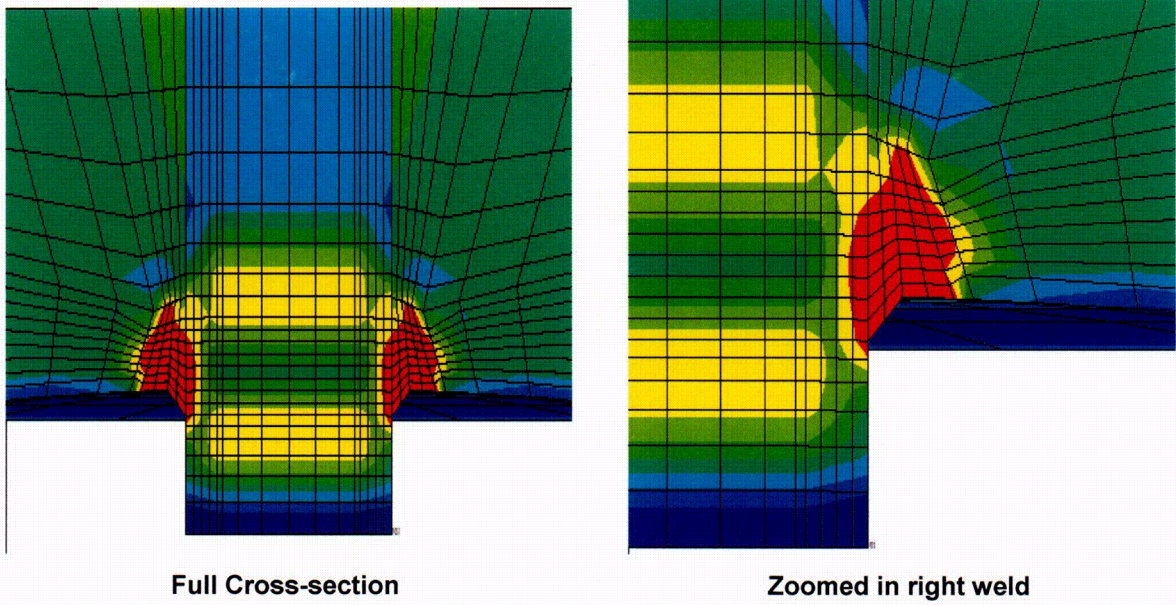


**Figure 4:** Hoop stress contours for the 0° nozzle. High tensile stresses occur in the weld and adjacent tube material. The bottom of the tube is in compression.

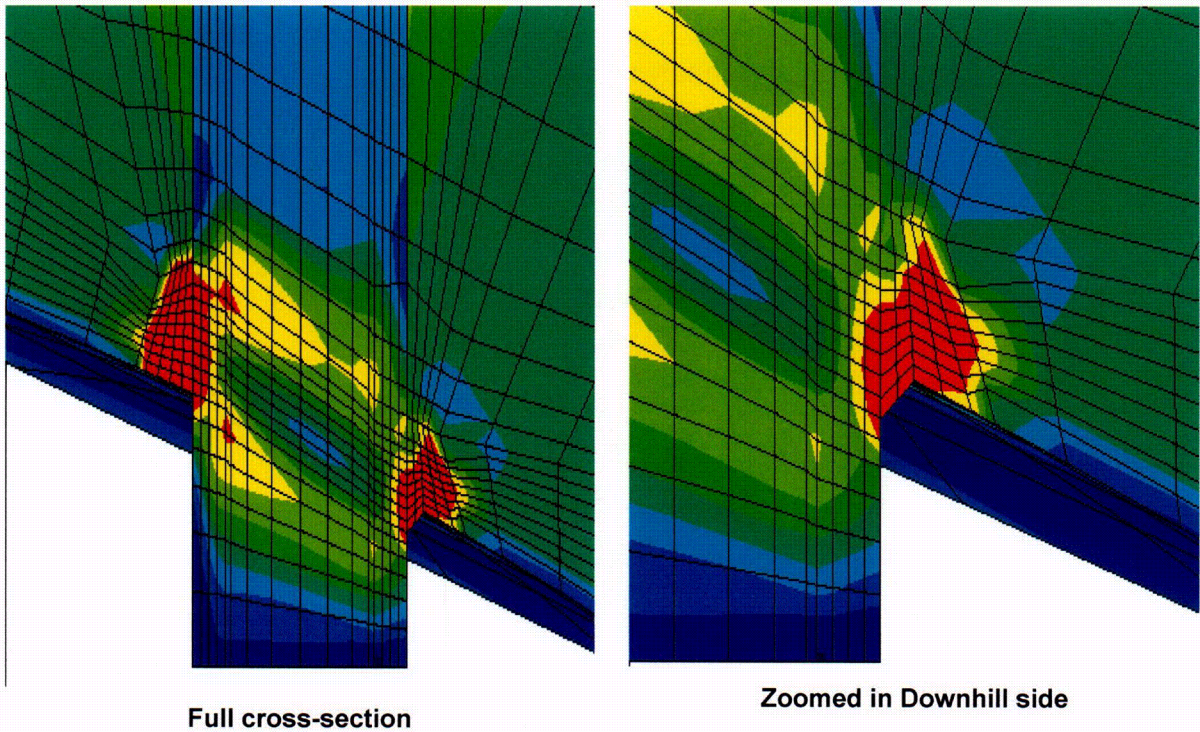
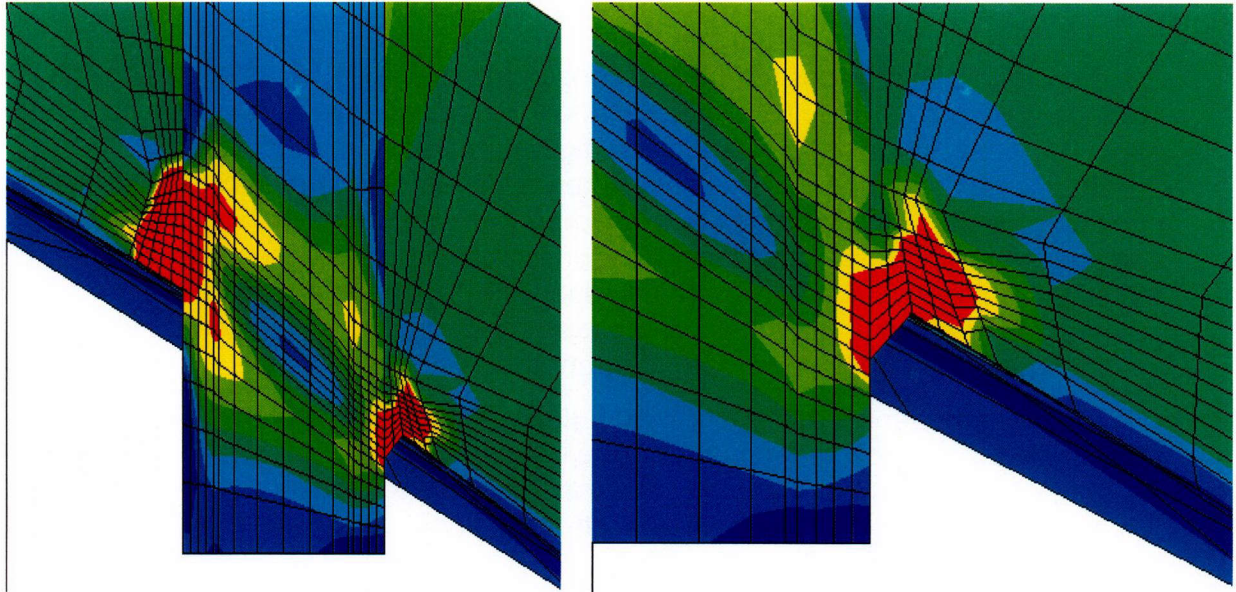


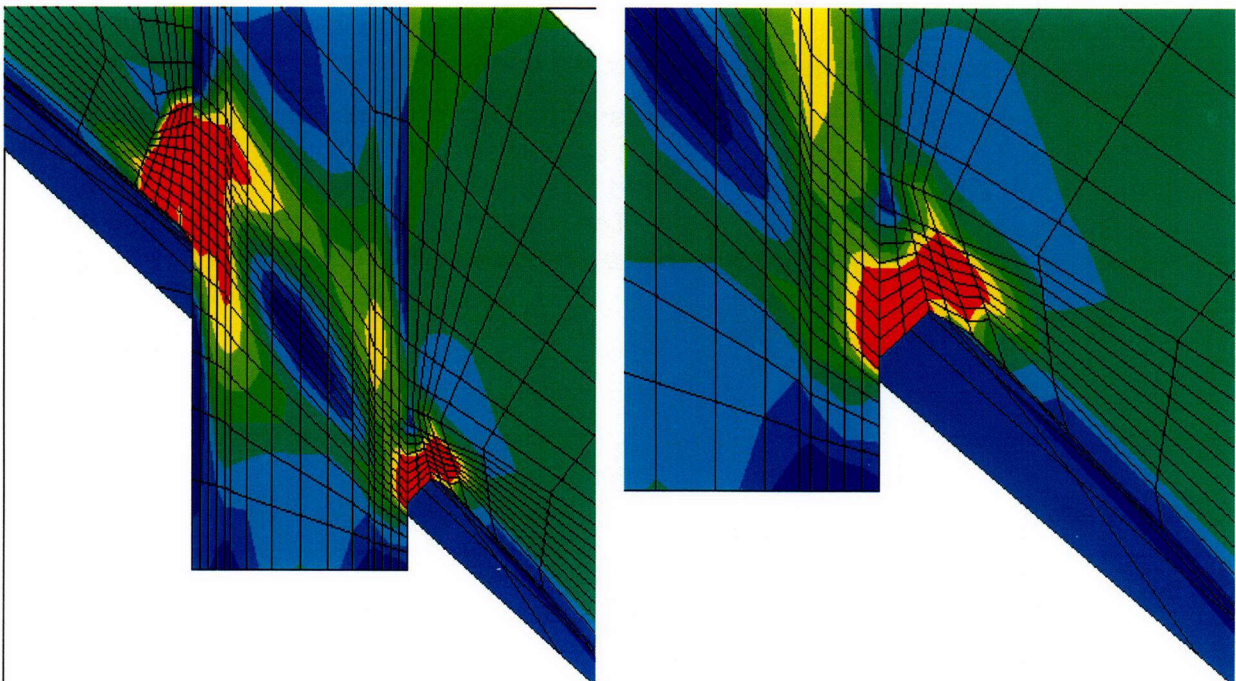
**Figure 5:** Hoop stress contours for the 18.2° nozzle. High tensile stresses occur in the weld and adjacent tube material. The bottom of the tube is in compression.



Full cross-section

Zoomed in Downhill side

**Figure 6:** Hoop stress contours for the 26.2° nozzle. High tensile stresses occur in the weld and adjacent tube material. The bottom of the tube is in compression.



Full cross-section

Zoomed in Downhill side

**Figure 7:** Hoop stress contours for the 38.5° nozzle. High tensile stresses occur in the weld and adjacent tube material. The bottom of the tube is in compression.

The nodal stresses for the locations of interest in each of the four nozzle groups were provided by Dominion Engineering Inc. and were tabulated in Reference 3b. The nodal stresses and associated figures representing the OD and ID distributions along the tube axis are presented in tables and associated figures in the following pages. The location of the weld bottom was maintained at the node row ending with "601". The blind zone location is shown on the associated figure. The three azimuthal locations downhill ( $0^\circ$ ), uphill ( $180^\circ$ ), and mid-plane ( $90^\circ$ ) are shown in the figures presented in the following pages. The zone of compressive stress is shown in the figure to be in the lower left quadrant that is bounded by the two dashed lines.

From the tables and associated figures, a full visualization of the stress distribution in the nozzle, from the nozzle bottom (located at 0.0 inch) to the J-weld is obtained. These figures are also shown in the Mathcad worksheets provided in the Appendix "C" attachments. The nodal stress distribution, provided by Dominion Engineering, is used to establish the region of interest and the associated stress distribution that will be utilized in the subsequent analyses. In the three nozzle groups ( $0^\circ$ ,  $18.2^\circ$  and  $26.2^\circ$ ) there exists a well defined compression zone. For the higher angle nozzle group ( $38.5^\circ$  at the mid-plane location) tensile stresses were found to exist at the nozzle bottom. Hence there was no well defined compression zone in this nozzle. In this particular case the tension stress magnitude was low ( $\sim 10.0$  ksi), and the distribution through the wall thickness had compressive stresses. For this nozzle location the presence of a low magnitude tensile stress on one surface is not expected to cause PWSCC initiation. However, this location was selected for further evaluation using deterministic fracture mechanics and is discussed in a later section.

In the following pages, the stress data from the Excel spreadsheet provided by Dominion Engineering (Reference 3b) and plots representing the axial distribution at the ID and OD locations are presented for each nozzle group with the specific azimuthal location that is evaluated. The location of the compression zone the blind zone and bottom of the weld are marked by colored reference lines.

Row	Height	ID	25%	50%	75%	OD
1	0.000	-30.99	-30.92	-31.719	-35.433	-35.967
101	0.441	-2.37	-4.15	-6.024	-7.411	-9.003
201	0.793	27.862	23.567	19.705	17.995	12.782
301	1.076	42.802	38.705	32.039	24.149	15.988
401	1.303	47.376	40.949	35.624	31.779	29.726
501	1.484	48.173	40.841	37.026	40.902	48.506
601	1.629	43.475	39.757	38.459	47.748	55.999
701	1.794	35.074	35.427	38.776	48.731	61.472
801	1.959	25.697	30.809	38.834	51.732	66.515
901	2.124	19.183	27.111	38.578	52.687	65.89
1001	2.288	18.854	25.754	38.057	52.967	65.445
1101	2.453	24.413	27.433	37.441	48.615	62.275
1201	2.618	31.382	31.231	36.808	46.394	54.749

**Table 2:** Nodal stress for 0° nozzle. This nozzle is symmetric about the nozzle axis hence these stresses prevail over the entire circumference. The weld location is shown by the shaded row.

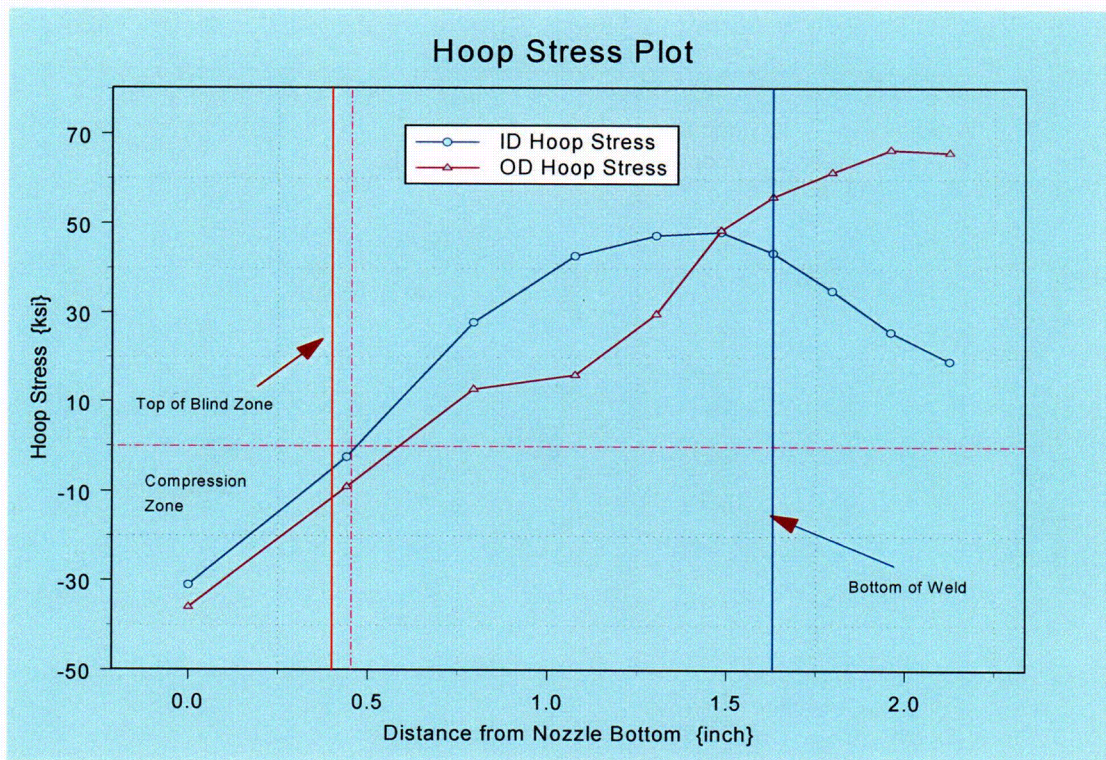


**Figure 8:** Plot showing hoop stress distribution along tube axis for the 0° nozzle. The compression zone, the top of blind zone, and the bottom of the weld are shown.

Row	Height	ID	25%	50%	75%	OD
1	0.000	-32.98	-29.552	-27.619	-25.631	-23.659
101	0.463	4.418	1.431	-2.622	-5.982	-7.485
201	0.834	23.603	20.133	17.472	13.58	8.558
301	1.131	39.381	33.757	28.588	23.549	16.901
401	1.369	41.077	35.596	32.564	29.095	28.069
501	1.560	35.472	35.035	34.721	41.389	51.476
601	1.712	25.309	30.935	36.756	48.633	57.324
701	1.854	18.476	26.759	37.578	49.667	67.274
801	1.996	15.182	24.435	37.506	53.17	72.592
901	2.138	16.043	22.797	36.698	51.389	59.83
1001	2.279	21.021	24.935	35.705	50.631	66.676
1101	2.421	26.705	26.535	36.109	44.384	53.376
1201	2.563	31.334	31.319	34.356	42.349	43.153

**Table 3:** Nodal stress for 18.2° nozzle at the downhill location. The weld location is shown by the shaded row.

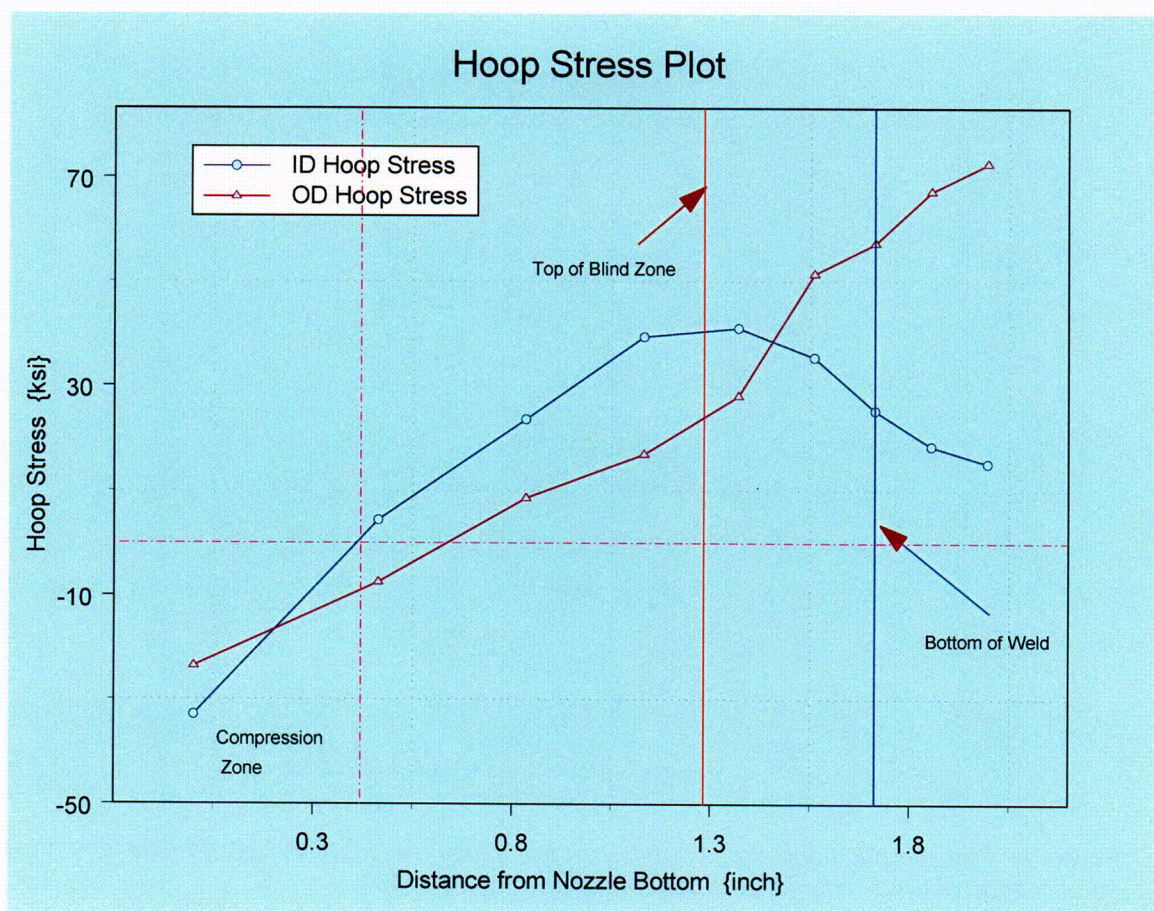


**Figure 9:** Plot showing hoop stress distribution along tube axis for the 18.2° nozzle at the downhill location. The compression zone, the top of blind zone, and the bottom of the weld are shown.

Row	Height	ID	25%	50%	75%	OD
80001	0.000	-15.271	-13.45	-13.143	-12.825	-12.103
80101	0.862	-1.538	-5.725	-10.568	-14.254	-17.443
80201	1.553	18.053	15.629	3.72	-8.133	-16.919
80301	2.106	35.538	34.972	26.87	5.376	-11.03
80401	2.549	46.071	44.442	37.478	23.453	13.214
80501	2.904	52.65	44.403	37.227	37.55	44.134
80601	3.189	48.6	42.887	42.714	56.058	66.098
80701	3.354	39.228	41.11	47.652	62.239	78.684
80801	3.520	31.415	39.177	50.091	65.872	77.544
80901	3.685	28.557	36.461	51.385	66.316	67.807
81001	3.851	30.354	37.802	51.087	65.419	76.035
81101	4.016	35.974	41.093	49.888	60.979	73.541
81201	4.182	42.147	43.54	46.913	55.231	65.515

**Table 4:** Nodal stress for 18.2° nozzle the uphill location. The weld location is shown by the shaded row.

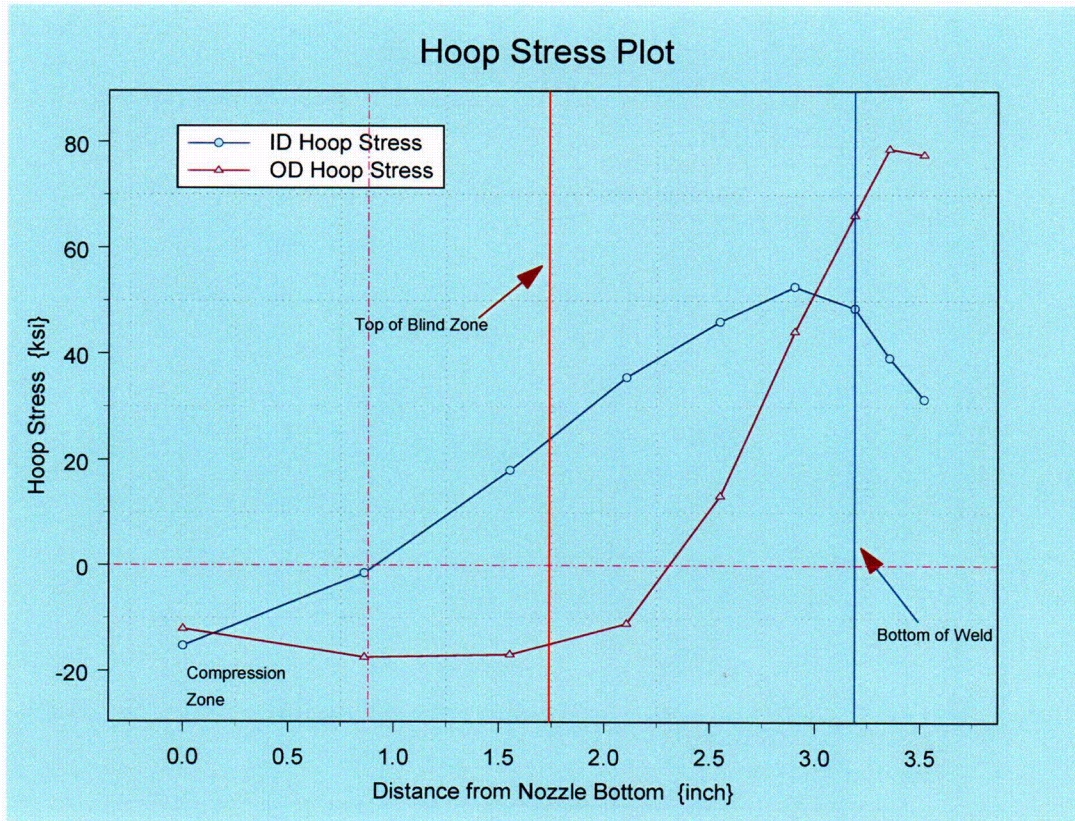


**Figure 10:** Plot showing hoop stress distribution along tube axis for the 18.2° nozzle at the uphill location. The compression zone, the top of blind zone, and the bottom of the weld are shown.

Row	Height	ID	25%	50%	75%	OD
40001	0.000	-15.876	-15.441	-15.26	-15.231	-15.607
40101	0.663	-2.577	-4.464	-6.327	-7.14	-7.152
40201	1.195	21.151	16.903	11.759	6.124	-0.117
40301	1.621	34.299	30.828	23.931	13.978	5.113
40401	1.962	39.982	32.343	27.07	23.686	19.206
40501	2.235	33.912	29.598	28.456	33.513	42.338
40601	2.454	22.125	26.126	29.581	43.075	54.179
40701	2.608	12.376	21.274	32.036	47.198	65.639
40801	2.761	7.853	19.169	32.443	49.488	67.334
40901	2.915	8.241	17.942	33.09	49.776	59.722
41001	3.069	12.022	20.283	32.869	47.255	62.581
41101	3.222	21.093	22.953	33.495	44.425	57.425
41201	3.376	29.386	27.197	32.222	42.642	50.772

**Table 5:** Nodal stress for 18.2° nozzle at mid-plane location. The weld location is shown by the shaded row.

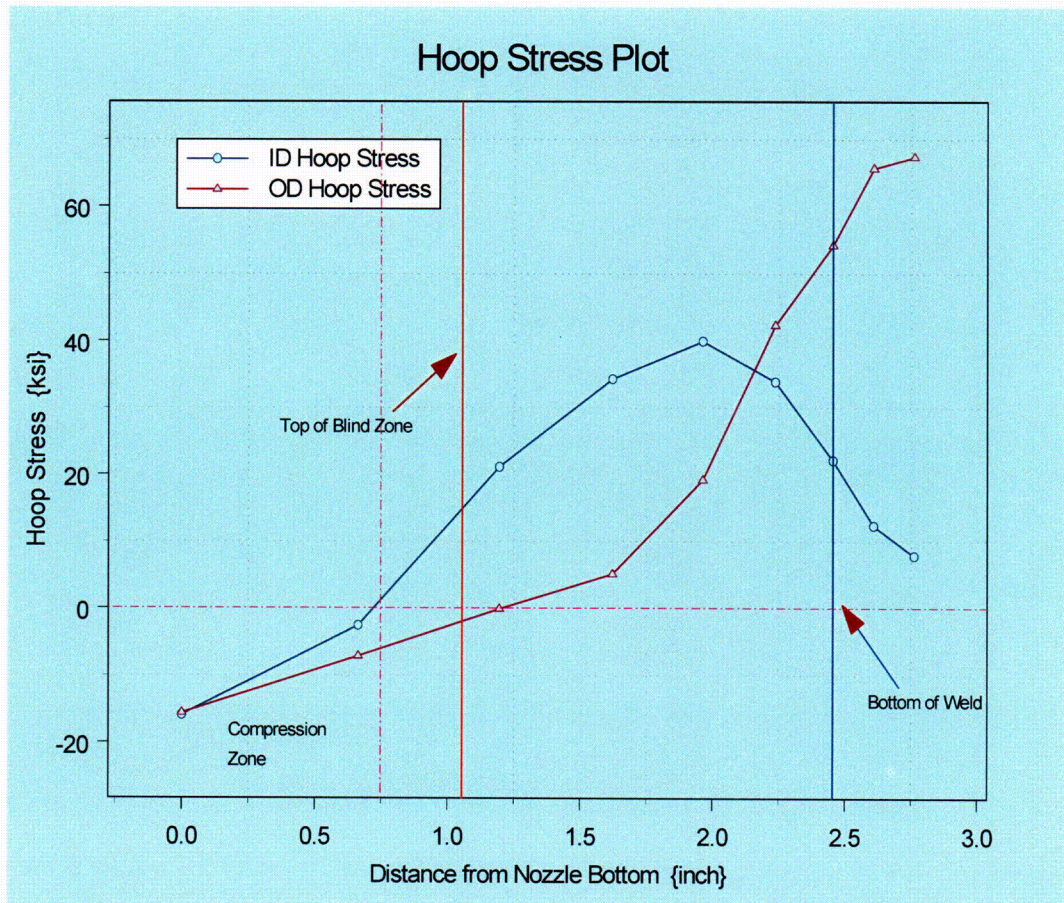


**Figure 11:** Plot showing hoop stress distribution along tube axis for the 18.2° nozzle at mid-plane location. The compression zone, the top of blind zone, and the bottom of the weld are shown.

Row	Height	ID	25%	50%	75%	OD
1	0.000	-30.999	-27.023	-25.148	-23.031	-20.485
101	0.428	4.34	1.335	-2.685	-5.687	-6.873
201	0.770	14.732	13.5	13.201	8.377	2.376
301	1.045	29.692	25.968	23.306	20.778	13.225
401	1.265	38.185	33.752	31.17	27.204	22.26
501	1.441	34.205	33.736	33.768	42.178	52.957
601	1.582	25.565	30.892	36.524	51.358	58.03
701	1.721	17.898	26.785	37.376	49.171	62.922
801	1.859	14.141	23.872	37.125	51.822	72.266
901	1.997	14.142	21.901	36.565	50.51	60.668
1001	2.136	18.477	23.68	35.651	50.883	68.048
1101	2.274	22.153	24.584	35.784	43.92	49.437
1201	2.412	26.389	29.517	31.718	38.942	34.145

**Table 6:** Nodal stress for 26.2° nozzle at the downhill location. The weld location is shown by the shaded row.

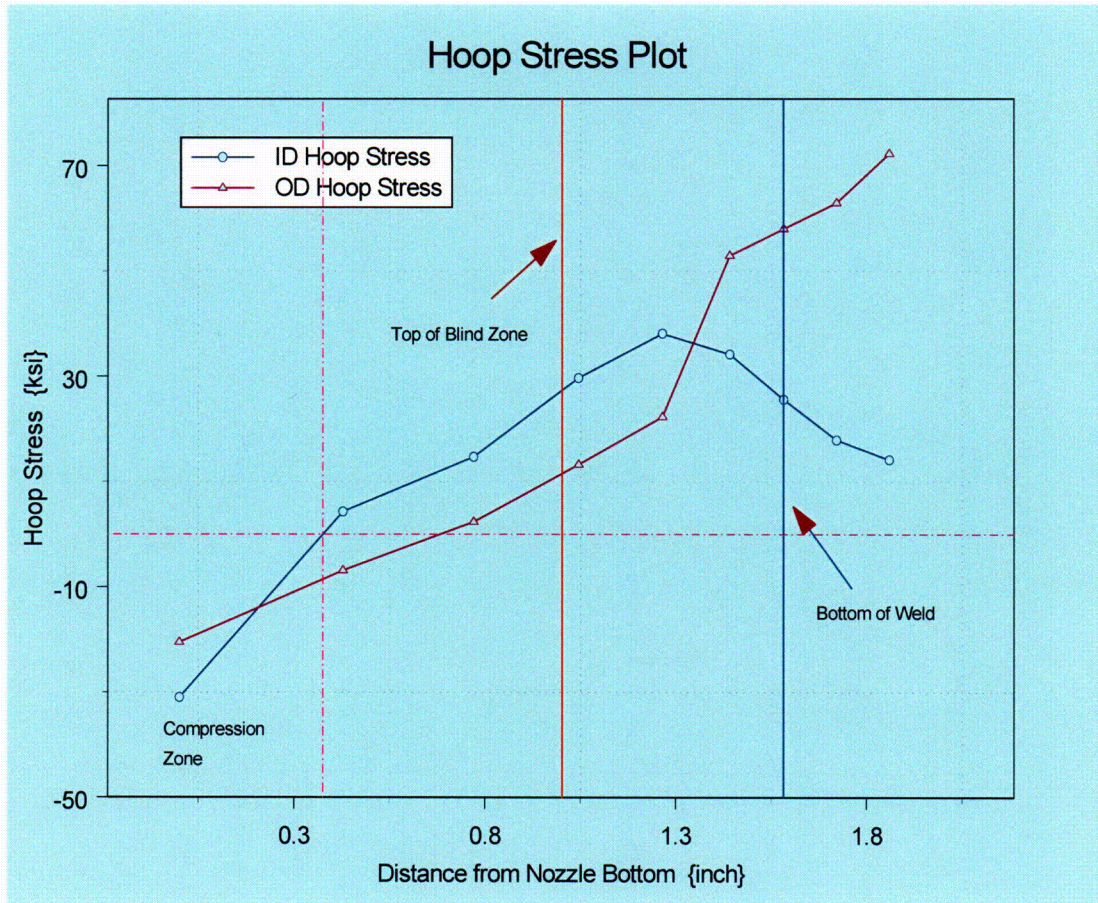


**Figure 12:** Plot showing hoop stress distribution along tube axis for the 26.2° nozzle at the downhill location. The compression zone, the top of blind zone, and the bottom of the weld are shown.

COG

Row	Height	ID	25%	50%	75%	OD
80001	0.000	-12.934	-10.204	-9.353	-8.617	-7.099
80101	1.025	0.519	-4.242	-9.482	-13.627	-17.298
80201	1.847	16.931	14.06	-0.789	-16.944	-24.212
80301	2.505	34.465	32.57	24.112	-3.745	-20.265
80401	3.032	45.126	44.235	39.085	19.069	5.15
80501	3.454	53.129	46.976	39.674	37.639	40.319
80601	3.793	53.097	46.566	45.522	57.594	62.505
80701	3.979	47.806	46.303	50.825	63.105	76.986
80801	4.165	40.475	46.132	54.308	68.334	76.803
80901	4.351	36.46	42.769	56.049	68.345	71.426
81001	4.537	35.844	42.789	56.287	69.758	77.424
81101	4.723	38.743	45.608	55.571	66.746	77.618
81201	4.909	44.155	47.881	52.527	61.191	71.097

**Table 7:** Nodal stress for 26.2° nozzle at the uphill location. The weld location is shown by the shaded row.

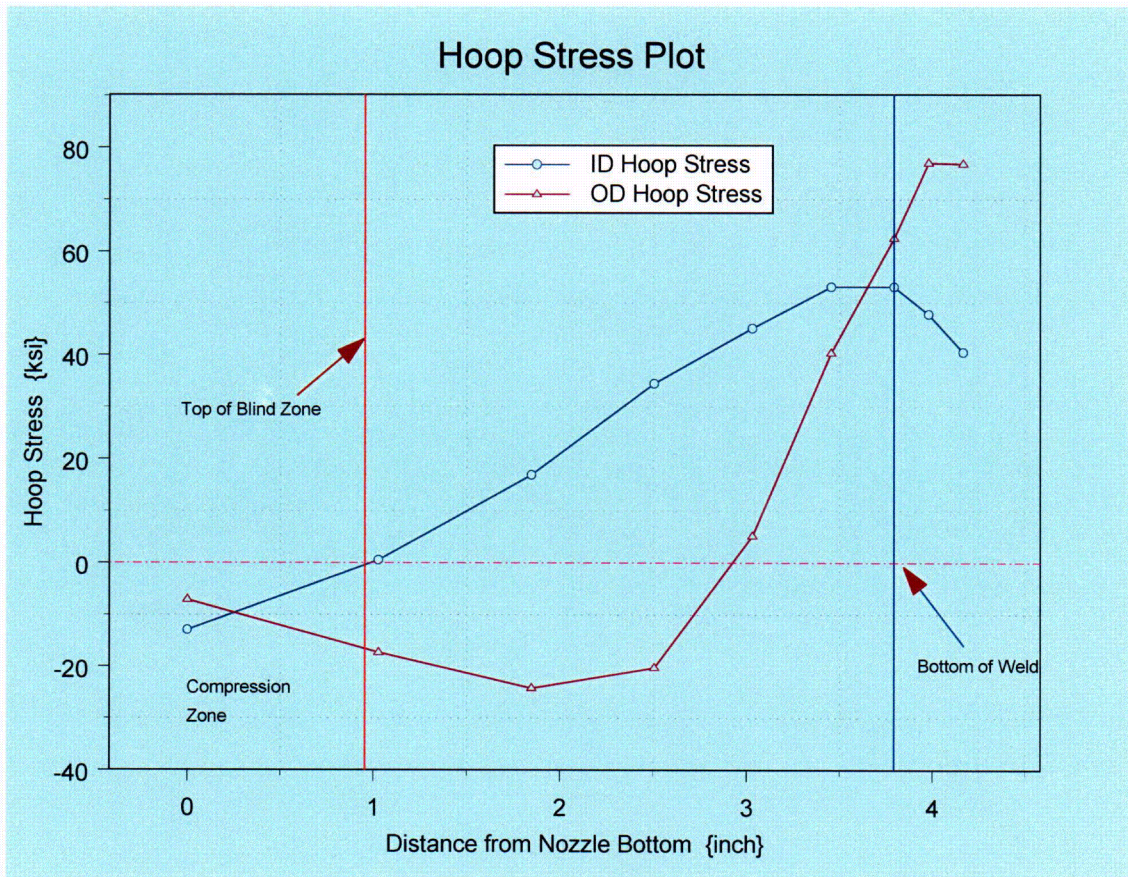


**Figure 13:** Plot showing hoop stress distribution along tube axis for the 26.2° nozzle at the uphill location. The compression zone, top of blind zone and the bottom of the weld are shown.

Row	Height	ID	25%	50%	75%	OD
40001	0.000	-4.881	-6.344	-7.277	-8.257	-9.768
40101	0.729	-3.137	-4.259	-5.323	-5.657	-5.284
40201	1.312	11.237	8.853	6.944	4.582	0.547
40301	1.780	26.997	23.318	18.343	11.84	5.76
40401	2.155	31.378	25.438	22.099	20.121	17.774
40501	2.455	24.259	22.52	23.163	29.696	38.662
40601	2.695	13.023	18.873	23.528	37.756	47.515
40701	2.858	3.329	13.248	24.402	40.285	56.577
40801	3.020	-1.382	11.182	24.275	42.021	57.851
40901	3.182	-1.269	9.685	25.303	42.043	53.218
41001	3.345	0.866	11.335	25.155	39.899	54.458
41101	3.507	10.022	13.661	26.854	38.58	50.621
41201	3.670	18.215	18.191	25.804	37.533	44.945

**Table 8:** Nodal stress for 26.2° nozzle at the mid-plane location. The weld location is shown by the shaded row.

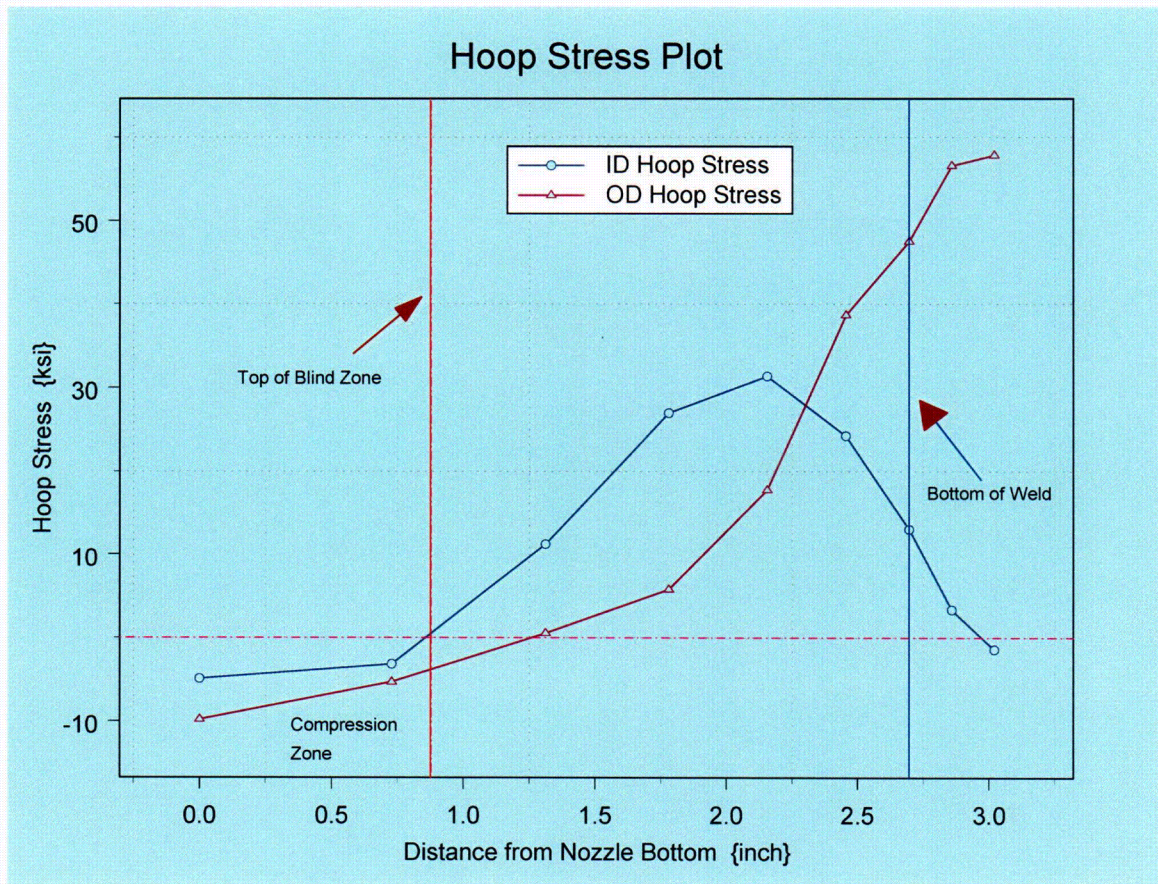


**Figure 14:** Plot showing hoop stress distribution along tube axis for the 26.2° nozzle at the mid-plane location. The compression zone, top of blind zone and the bottom of the weld are shown.

Row	Height	ID	25%	50%	75%	OD
1	0.000	-27.262	-26.568	-25.018	-20.841	-15.546
101	0.355	-8.663	-3.917	-2.294	-3.371	-2.704
201	0.640	1.497	3.941	8.574	6.533	3.174
301	0.868	18.44	16.972	16.875	13.139	6.557
401	1.051	27.564	27.006	28.041	24.607	19.607
501	1.198	24.021	27.991	34.116	49.117	53.8
601	1.315	18.785	26.702	37.396	54.727	56.187
701	1.463	17.64	25.575	39.708	56.365	66.86
801	1.610	19.157	26.134	38.392	55.373	77.311
901	1.758	21.403	25.014	37.324	51.052	66.312
1001	1.906	27.58	28.743	35.137	47.213	67.591
1101	2.054	25.638	27.624	34.486	37.362	41.426
1201	2.202	32.346	32.663	26.936	27.922	21.797

**Table 9:** Nodal stress for 38.5° nozzle at downhill location. The weld location is shown by the shaded row.

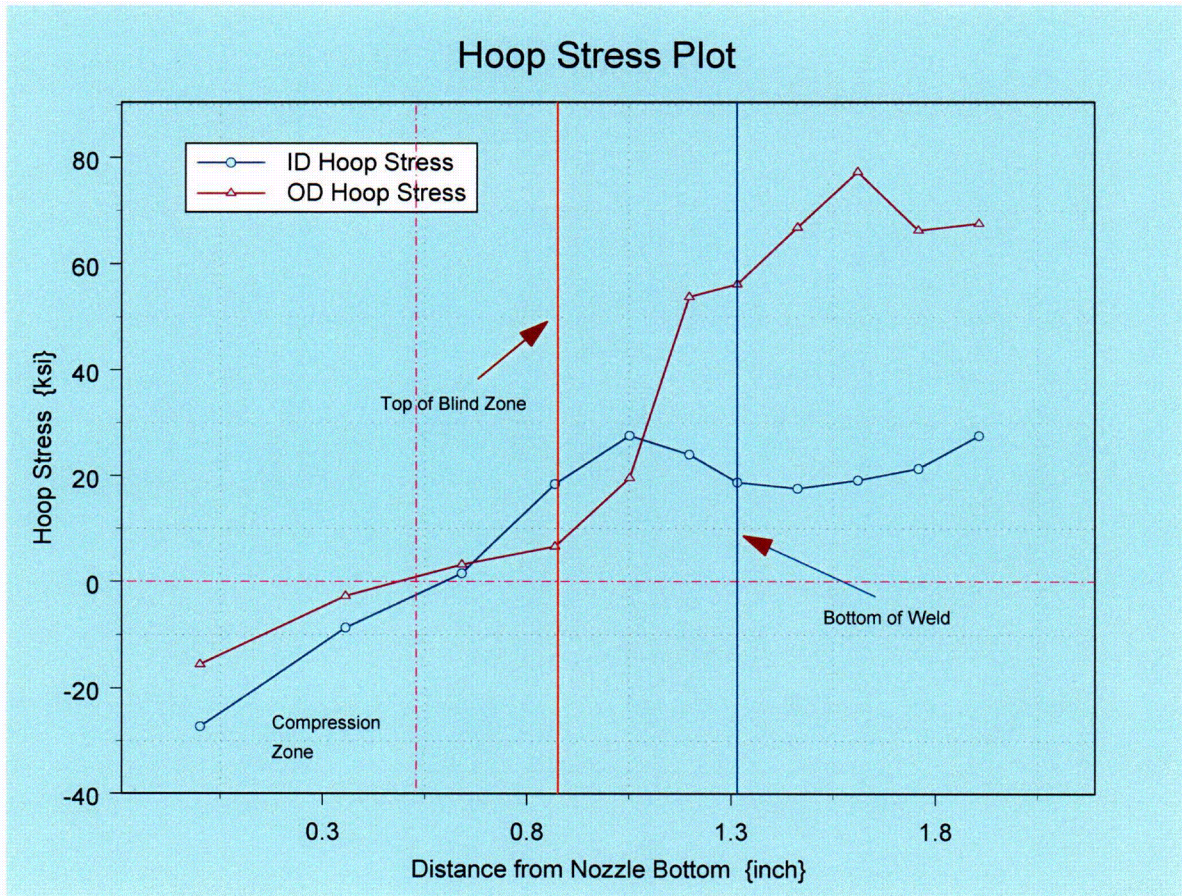


**Figure 15:** Plot showing hoop stress distribution along tube axis for the 38.5° nozzle at downhill location. The compression zone, top of blind zone and the bottom of the weld are shown.

Row	Height	ID	25%	50%	75%	OD
80001	0.000	-20.713	-13.891	-10.091	-6.781	-2.467
80101	1.324	5.79	-0.121	-6.365	-11.555	-16.261
80201	2.385	20.088	19.42	1.112	-21.708	-29.318
80301	3.235	35.237	33.451	21.848	-18.777	-33.482
80401	3.916	46.802	45.156	37.936	8.372	-15.972
80501	4.461	51.852	48.945	42.423	37.185	32.638
80601	4.898	55.053	50.07	49.796	57.893	55.558
80701	5.119	55.224	51.157	55.733	63.865	70.724
80801	5.340	53.096	55.783	60.808	70.802	73.937
80901	5.561	50.453	53.108	62.734	69.701	72.988
81001	5.782	48.972	52.732	63.772	74.803	79.068
81101	6.003	48.085	53.86	65.077	74.976	82.011
81201	6.224	50.67	55.952	62.826	70.744	77.451

**Table 10:** Nodal stress for 38.5° nozzle the uphill location. The weld location is shown by the shaded row.

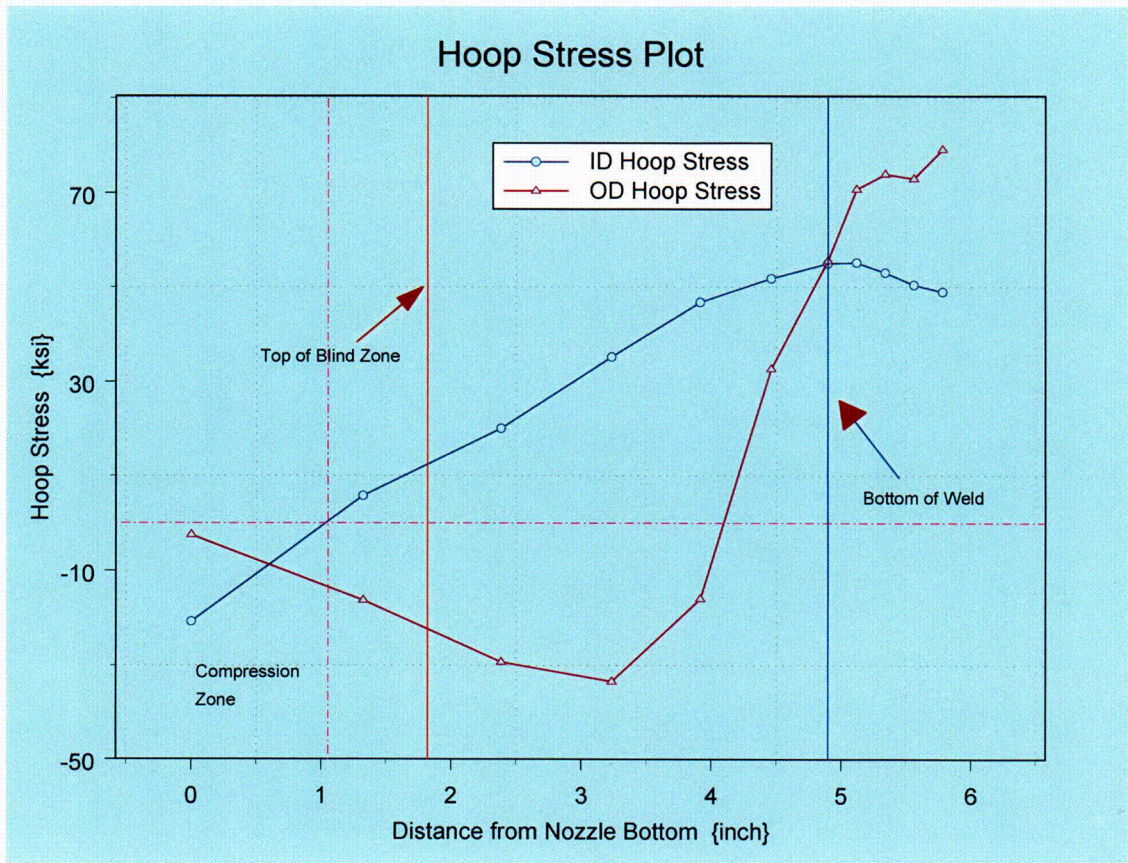


**Figure 16:** Plot showing hoop stress distribution along tube axis for the 38.5° nozzle at the uphill location. The Compression zone, top of blind zone and the bottom of the weld are shown.

Row	Height	ID	25%	50%	75%	OD
40001	0.000	10.954	4.51	0.522	-3.322	-7.653
40101	0.846	1.32	-0.955	-2.652	-3.103	-3.549
40201	1.524	4.766	4.123	5.007	4.329	1.791
40301	2.067	15.552	13.981	12.901	10.287	7.177
40401	2.502	15.655	12.983	14.758	16.943	17.57
40501	2.851	4.83	8.828	13.891	24.741	33.61
40601	3.130	-7.464	3.508	12.564	30.987	40.998
40701	3.315	-16.1	-2.811	11.744	31.306	44.814
40801	3.500	-19.775	-4.84	10.363	31.622	44.873
40901	3.685	-18.205	-5.805	11.632	30.03	40.103
41001	3.870	-16.362	-3.949	11.963	27.256	40.737
41101	4.055	-6.523	-1.62	14.387	27.003	37.168
41201	4.240	1.577	4.361	14.559	27.38	32.59

**Table 11:** Nodal stress for 38.5° nozzle at the mid-plane location. The weld location is shown by the shaded row.

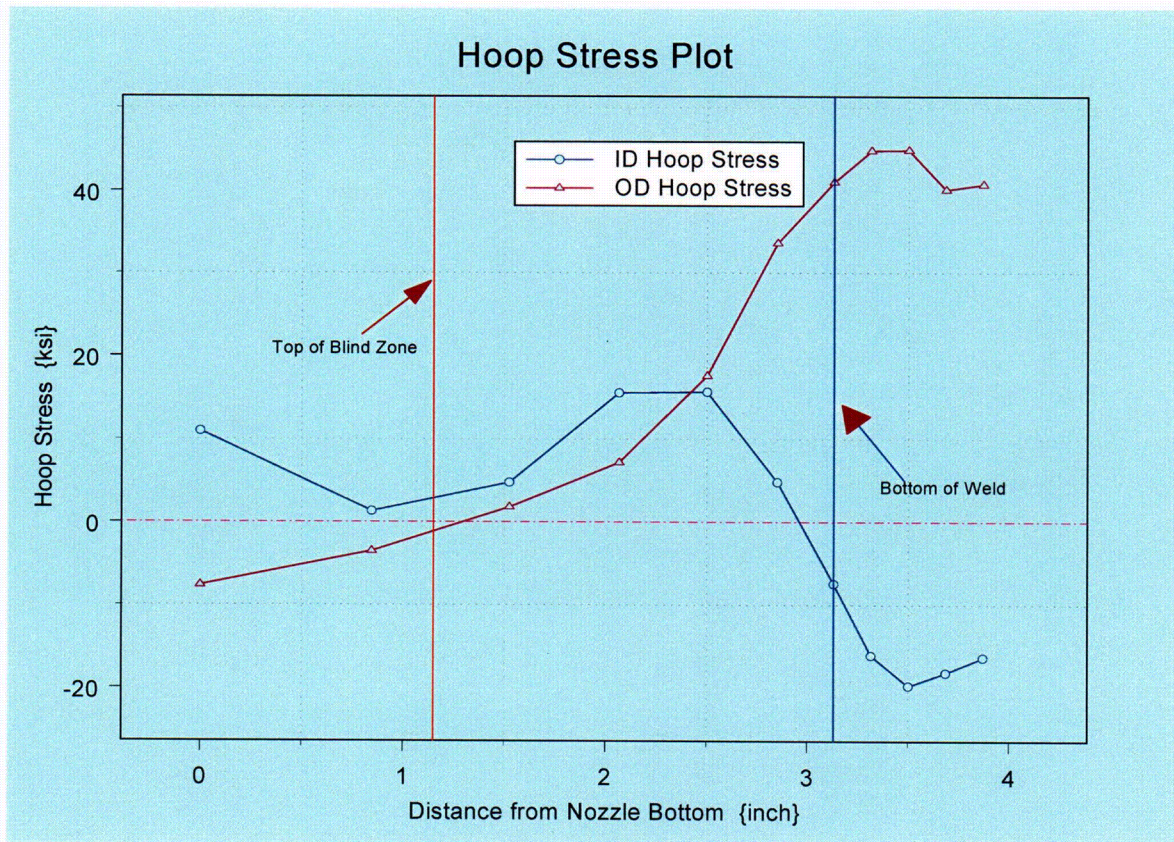


**Figure 17:** Plot showing hoop stress distribution along tube axis for the 38.5° nozzle at the mid-plane location. The top of blind zone and the bottom of the weld are shown. No compression zone exists because the ID surface has a 10.954 ksi tensile stress.